Observational evidence of change in extreme wind along the Eastern Seaboard of the United States

A thesis submitted by

Jai Seoung Chung

in partial fulfillment of the requirements for the degree of

Master of Science

in

Civil and Environmental Engineering

Tufts University

February 2018

Adviser: Laurie Baise

Abstract

Extreme winds cause significant damage to infrastructure in the United States. Climate change effects to extreme winds including increasing trends have been predicted in climate change scenarios; however, little observational evidence exists to support the hypothesis of increasing winds in U.S. coastal communities due to climate change. In this study, we use the historical record of peak 3-s gust winds at sites along the Eastern Seaboard to determine if nonstationarity exists in the historic wind record. We evaluate nonstationarity at individual stations and within regional "superstation" clusters. In order to evaluate nonstationarity, both parametric (Student's t-test) and non-parametric (Mann-Kendall) trend tests are used. As Lombardo and Ayyub (2014) separated winds by storm types, we observe evidence of nonstationarity by storm types (commingled, nonthunderstorms, thunderstorms and tropical storms). For commingled data, 23 out of 108 stations exhibit evidence of nonstationarity. Roughly 16% of these stations show a positive trend from Florida to NY. In New England, 6% of stations exhibit a negative trend.

In addition to the single station results, we cluster similar wind sites together using the *k*-means algorithm, to extend observation records and observe nonstationary behavior of extreme winds regionally. Incorporating L-moments in regional frequency analysis for clustering purposes requires regional standardized L-moment parameters (Eslamian et al., 2012; Parida et al., 1998). A combination of three parameters consisting of latitude, longitude and L-CV is used to define the *k*-means clustering. Regional frequency analysis (Hosking and Wallis, 1997) is carried out using L-moments to confirm homogeneity of the cluster prior to evaluation of nonstationarity. Once the clusters are defined, we employ the "superstation" (Peterka, 1992; Peterka and Shahid., 1993) method for each cluster to extend and regionalize the record. By

creating a virtual “superstation”, we have a single database with extended records and reduced sample errors. Using trend tests, we find evidence of statistically significant regional nonstationarity of 3-s gust wind speeds in 4 out of 7 clusters, all resulting in a positive trend. Two clusters are in Florida, one is along the mid-coast and the final one is New Englnad. The cluster in New England exhibits heterogeneity according to the L-moment homogeneity tests. The trend tests for three of the regional clusters do not exhibit a statistically significant trend. For the two statistically significant clusters in Florida, we apply a nonstationary homoscedastic trend model to identify return levels with time of interest at years 2010, 2030, 2050.

Acknowledgements

I am indebted to the mentors, teachers, professors and friends who have supported me and helped me during my graduate school career. I am thankful to my advisor, Laurie Baise, who has guided me for the course of this research. While wind was a rather unfamiliar topic to both of us, under her supervision I was able to overcome such obstacles. I am also indebted to my other committee members: Richard Vogel, who has been patient on teaching me from the basics of statistics and how to interpret results, Franklin Lombardo, who has been kind of enough to share the 3-s peak gust wind data, and Jonathan Lamontagne, who provided further feedback on my methodology of my thesis. I am also grateful to my 308F office mates (Vahid, Jing, Gerrit, Marshall and Mark), who have always been supportive.

Last but not least – I have been, I am, I will be always grateful to my parents for their love and support.

This work would not have been possible without funding from the National Science Foundation (1455450).

Table of Contents

List of Tables

List of Figures

Introduction

Extreme winds can cause significant damage to infrastructure. Some climate change scenarios for the U.S. have predicted increasing trends in extreme winds (Young et al., 2011). However, little observational evidence exists to support the hypothesis of increasing winds in US coastal communities due to climate change. The proposed work is an observational study of extreme winds along the Eastern Seaboard of the United States.

Steenbergen et al. (2012) predicts a change of -1% to +4% of the annual minimum and maximum daily mean wind speeds in the Netherlands for 2050 using four possible climate change scenarios presented by Royal Netherlands Meteorological Institude (KNMI) (Van den Hurk et al., 2006). In addition, the study suggests that for buildings to have a certain level of safety during the intended life-time, building standards must consider future trends in wind speeds. Infrastructure is historically designed assuming a stationary climate; however, including a trend in wind speeds in design would provide a design that considers impacts of climate change (Klein Tank et al., 2009). In general, present-day building codes and government planning agencies do not consider issues related to nonstationarity from a climate change perspective. Buildings have been threatened by evident indicators (e.g. flood risk) of climate change since the 20^{th} century (Hamlet and Lettenmaier, 2007; Ten Brinke et al., 2008) and awareness of these issues is increasing. As evidence of climate change gains recognition, researchers and scientists need to quantify impacts of climate change, including extreme wind speeds. While the focus for infrastructure has been on flood risk (Rosner et al., 2014), this study examines observational evidence of nonstationarity in extreme winds.

In the context of extreme winds, Nishijima et al. (2012) quantified wind risk of residential buildings in Japan by simulating future climates using the atmospheric general

circulation model (AGCM). Mudd et al. (2015) assessed climate change impact on the East Coast of the US through projected hurricanes in climate change scenarios; for example, the study identifies that the design wind speed will be exceeded under climate scenario RCP 8.5 in the year 2100 across the East Coast. Knutson and Tuleya (2004) used Coupled Model Intercomparison Project (CMIP2+) climate models to show small increases in future wind speeds as result of climate change along with global warming. The Intergovernmental Panel on Climate Change expect the frequency and intensity of extremes to fluctuate in the future (Solomon et al., 2007). Each of the studies that predict wind speed increases rely on atmospheric climate change scenarios. In contrast from observational data, Vautard et al. (2010) have shown evidence of atmospheric stilling in the Northern Hemisphere due to an increase in surface roughness -- annual mean wind speeds decreased at 73% of surface sites. Lombardo and Ayyub (2014) separated winds in the Baltimore-Washington metropolitan area by storm types and observed downward trends in the region; however, it suggested that future projection of extreme wind speeds to be difficult primarily due to nonclimate factors. Therefore, there is an open question concerning observational evidence of nonstationarity in extreme wind records.

In the proposed work, wind recording sites that observed peak 3-s gust wind data along the Eastern Seaboard over the past 40 years are used to evaluate nonstationarity (Hosking and Wallis, 1997; Reed et al., 1999). Nonstationarity is evaluated both at single stations and by clustering stations within regional superstations. The “superstation” approach was introduced by Peterka (1992), which combines wind records of sites across a region resulting in longer records and a decrease in sampling errors. Wind recording sites across a region that share similar characteristics are identified as a cluster through cluster analysis. Several climatological studies have applied superstation methodology via cluster analysis (Goel et al., 2004; Erfani et al., 2016;

Hong and Ye, 2014). However, regional frequency analysis must be carried out beforehand to check for discordancy and homogeneity of the measuring sites to insure a homogeneous region or station cluster.

Cluster analysis is a prevalent technique among climate studies (Darby, 2005; Wolter, 1987; Kaufmann & Whiteman, 1999; Satyanarayana & Srinivas, 2008) to classify similar recording sites. Of the cluster analysis methodologies that exist, we apply the *k*-means analysis; *k*-means analysis is the most widely applied method because of a) its simplicity and b) its iterative mechanism that reassigns observations as it tries to fulfill the objective function. A disadvantage of the *k*-means analysis is that a specific number of clusters, *k*, needs to be assigned a priori. For our study, *k*-means cluster analysis is performed with a combination of variables consisting of physical variables (latitude, longitude, elevation, nearest distance to shore, angle of nearest distance to shore) and wind variables (coefficient of variation, L-CV, L-Skewness, L-Kurtosis). After testing many combinations, we chose latitutde, longitude, and L-CV which is consistent with Hong and Ye (2014) which is a regional extreme wind study in Canada.

To characterize nonstationary behavior, trends must be detected from existing time series observations using parametric (Student's t-test) and nonparametric (Mann-Kendall test) Null-Hypothesis Significance Testing (NHST). Several studies have demonstrated methods for trend analysis for different types of annual extreme natural phenomena such as maximum temperature, precipitation and flood flow detection (e.g. Cheng et al., 2014, Vogel et al., 2013, Rosner et al., 2014, Pujol et al., 2007). Cheng et al. (2014) identified a significant trend on annual maximum temperature spatially using the Mann-Kendall trend test on observation sites around the world. Pujol et al. (2007) also identified a significant trend on annual maximum precipitation using the Mann-Kendall test. Hecht (2016), Vogel et al. (2013) and Rosner et al. (2013) identified whether

a nonstationary flood trend is apparent or not on annual maximum flood series using Student's t-test.

In this work, we use parametric (Student's t-test) and nonparametric (Mann-Kendall test) NHST for nonstationarity both at single stations and regional station clusters. We aim to address the following question: does nonstationarity exist in the observed 3-s peak gust record at sites and within regional clusters along the Eastern Seaboard? Answering this question will help us understand the behavior of extreme winds and will be of value in regionally assessing extreme winds.

Data

Observed peak 3-s gust wind data were originally recorded and archived by the National Oceanic and Atmospheric Administration (NOAA) website. Data have been converted to standardized 3-s gust wind speed at 10 m height as the measurement heights and instrumentations changed over the course of the records (Lombardo 2012). The region of interest for this study, the Eastern Seaboard, was defined between the ASCE 7-10 hurricane prone boundary (Figure 1) and the Atlantic Ocean. For this study, annual maximums of peak 3-s gust wind data from sites within the region of interest were considered to evaluate nonstationarity in extreme winds. The record length of annual maximum peak 3-s gust wind data differs by station site and by wind type. By using sites with at least 18 years of recorded data (5 years for tropical storms), a total of 108 sites for commingled and non-thunderstorms, 99 sites for thunderstorms and 117 sites for tropical storms were identified. While for majority of the commingled, non-thunderstorms and thunderstorm data are continuous, it is not the case for tropical storms. Tropical storm data are

limited and are often not continuous. Table A.1-4 shows each station, including latitude, longitude, and record length (by storm type).

Figure 2 shows an example record from Jacksonville Executive at Craig Airport station (KCRG) in Florida. In addition to examining the annual maximum time series of 3-s gust wind for each site, it is also recommended by (Lombardo and Ayyub 2014) that wind data should be examined by storm type. Figure 2 also shows the time series for KCRG station for each storm type (non-thunderstorm, thunderstorm, and tropical) along with the original commingled record. Along with the time series, a linear trend model is shown as discussed in Trend Significance section below. The wind v is shown as ln (v).

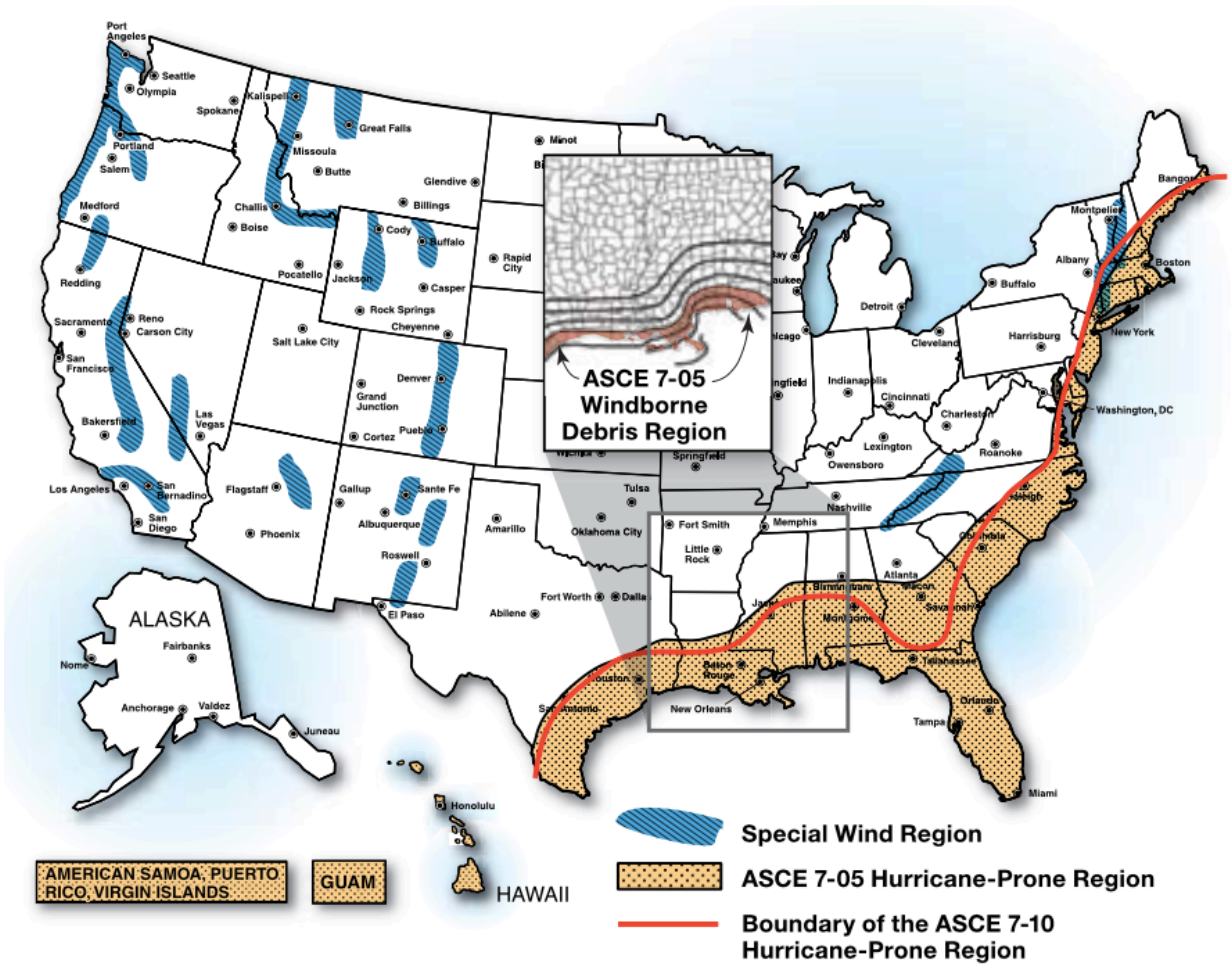

Figure 1. Illustration of the hurricane-prone region of the United States (Source: FEMA P-804)

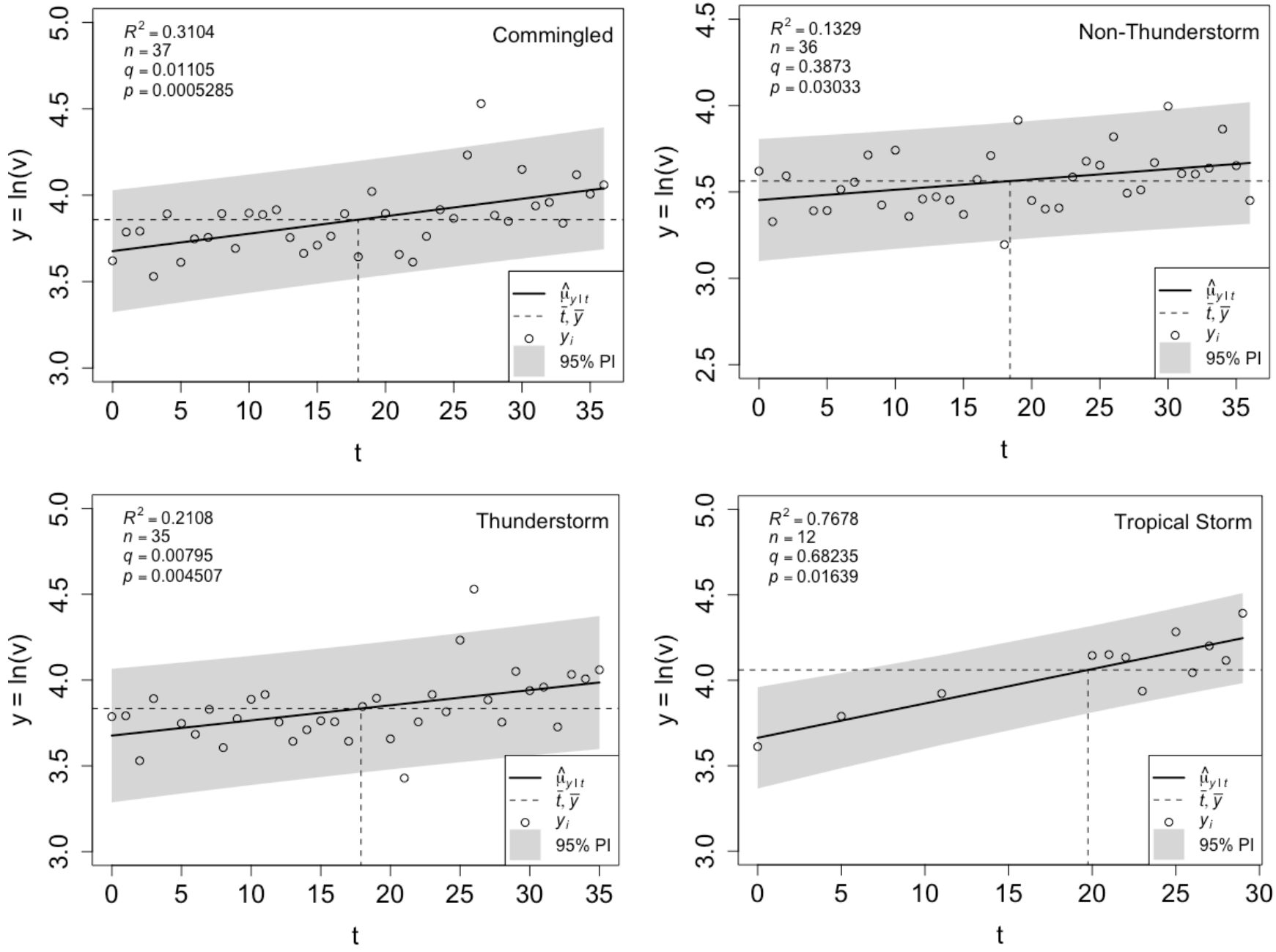

Figure 2. Regression Plots of Jacksonville Executive at Craig Airport by storm types

Studies have shown that extreme winds are well characterized by the lognormal distribution (LN2); for example, Morgan et al (2010) showed that the LN2 model performs best for estimating offshore extreme wind speeds and Huang (1999) showed that the LN2 model provides a better fit on simulated 50-year maximum extreme wind speeds for all sites in Southeastern United States compared to extreme value distributions. We use L-moments to verify the probability distribution for the annual maximum peak 3-s gust wind data.

L-moments, first introduced by Hosking (1990), are quantitative measures originating from modifications of the probability weighted moments (PWMs) of Greenwood et al. (1979). L-moments are used to describe a probability distribution and have been prevalently used in the field of regional frequency analysis. Compared to conventional moments, L-moments are superior descriptors of probability distributions and are also resistant to outliers (Vogel and Fennessey, 1993). The mathematical formulation of L-moments is as follows:

$$\lambda_1 = \beta_0 \tag{1}$$

$$\lambda_2 = 2\beta_1 - \beta_0 \tag{2}$$

$$\lambda_3 = 6\beta_2 - 6\beta_1 + \beta_0 \tag{3}$$

$$\lambda_4 = 20\beta_3 - 30\beta_2 + 12\beta_1 - \beta_0 \tag{4}$$

and β_i is given by

$$\beta_i = \frac{1}{n}\sum_{j=i+1}^{n} \frac{(j-1)(j-2)\cdots(j-i)}{(n-1)(n-2)\cdots(n-i)} x_{j:n}, \text{ for i} = 0, 1, 2, \ldots \tag{5}$$

where $x_{j:n}$ is denoted as the j-th ordered sample (in ascending order) of a set of samples of size n. Analogous to product moment ratio estimators (i.e. coefficient of variation C_v, skewness γ, and kurtosis κ), L-moments are standardized as higher moments as well, and are defined as

$$\tau_n = \lambda_n/\lambda_2, \text{ for n} = 3, 4, \ldots \tag{6}$$

Figure 3 shows the L-moment diagrams (L-CV vs. L-Skewness) for annual maximum 3-s peak gust wind data by storm type. The majority of sites for commingled, non-thunderstorms and thunderstorms are clustered near the LN2 curve as compared to the other distribution curves. The scatter around the curve is expected and a result of sample size – the larger the sample size, the lower the scatter. For tropical storms, the sites plot more broadly around the LN2 – this is due to the fact that sample L-moments have been calculated using lower number of samples. We can therefore assume for our study that the annual maximum 3-s peak gust wind data can assume to follow a LN2 distribution.

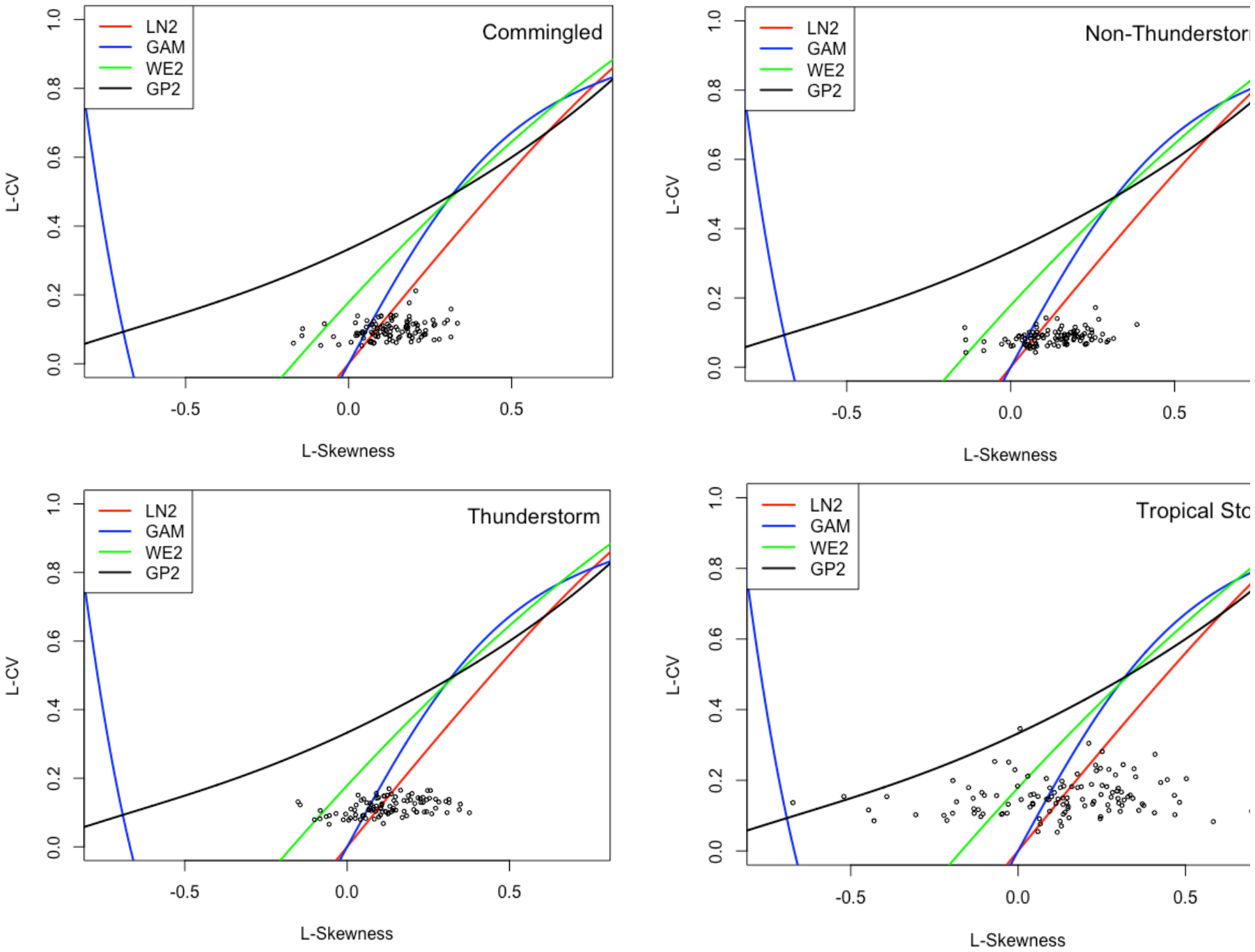

Figure 3. L-moment diagrams of annual maximum 3-s peak gust wind data series by storm types

Methodology

The trend test is a very important step in examining the stationarity of time series. In this work, the trend of individual sites is determined using the Student's t-test (Rosner et al., 2014) or the Mann-Kendall (MK) test (Mann 1945; Kendall 1975). The Student's t-test, which was first developed by William Sealy Gosset, is a parametric test that can be used to identify whether a linear trend in statistically significant. The MK test, as recommended by the WMO (World Meteorological Organization) (WMO 1988), is used to identify the significance of monotonic trends in hydrological series. However, the MK test generally has the advantage over the Student's t-test because it is non-parametric, i.e. it does not require distribution assumptions in the data while it maintains the same power as its parametric alternatives. Both trend tests are done to check the accordance of trend test statistics for each site; however, the results of the MK test are given priority in determining whether a trend is significant or not.

Prewhitening

The MK test has been shown that it is sensitive to autocorrelation structure in the time series (Kumar et al., 2009). It is therefore essential to pre-whiten sites with time series that show lag-1 autocorrelation within the 5% significance level. For pre-whitening, recommendations of von Storch (1999) will be followed in this study with

$$Y_t = X_t - r_1 X_{t-1} \text{ for } \mathrm{t} = 2,3, \ldots \quad (7)$$

where X_t is the original time series, r_1 is the lag-1 autocorrelation coefficient and Y_t is the pre-whitened time series. Subsequently, the MK test statistic will be calculated for the pre-whitened time series. The time series for KCRG station as shown in Figure 2 is prewhitened.

Trend Significance

Time series data from individual sites or clusters are evaluated to identify trend. The ordinary simple linear regression is applied to the time series of annual maximum peak 3-s gust wind data:

$$y = \beta_0 + \beta_1 t + \varepsilon \tag{8}$$

where y is defined as the logarithmic transformation of annual maximum peak 3-s gust wind data series as $y = \ln(v)$, β_0 is the intercept term of y, β_1 is the coefficient for the trend term, t is the time in year and ε is the error term.

One of the NHST trend tests that will be used in the study is the Student's t-test and it is a parametric trend test. Test statistics used for the Student's t-test are computed as (8) is applied for the linear regression of the annual maximum peak 3-s gust wind data series. The estimated slope coefficient, $\hat{\beta}_1$, is a test statistic used to assess a positive or a negative trend in the mean of the response variable, time (Haan, 2002; Kundzewicz and Robson, 2004). The null hypothesis, H_0, is when there is no linear trend (i.e. $H_0: \hat{\beta}_1 = 0$). For the trend test using Student's t-test, we compute significance statistics such as Type-I and Type-II error probabilities. The Type-I error probability, α, is estimated using

$$\alpha = P[T_{n-2} \geq t] \tag{9}$$

where T_{n-2} is Student's t random variable with $n-2$ degrees of freedom and $t = \hat{\beta}_1 / \hat{\sigma}_{\hat{\beta}_1}$ where $\hat{\sigma}_{\hat{\beta}_1}$ is the standard deviation of the estimated trend coefficient $\hat{\beta}_1$. Type-II error probability, β, is estimated using

$$\beta = P\left[T_{n-2} \leq (t_{1-\alpha,n-2} - \delta n^{0.5})\right] \tag{10}$$

where $\delta = \sqrt{\rho^{-2} - 1}^{-1}$, where ρ is the Pearson product moment correlation coefficient between variables x and y is defined as:

$$\rho = \frac{\sum_{i=1}^{n}(x_i - \bar{x}) \cdot (y_i - \bar{y})}{\sqrt{\sum_{i=1}^{n}(x_i - \bar{x})^2 \cdot \sum_{i=1}^{n}(y_i - \bar{y})^2}} \tag{11}$$

Per the definition of NHST, a low Type I error (i.e. < 0.05) implies that if there were no trend, there is a low chance we would conclude that a trend exists. Vice-versa, a high Type-I error is also associated with "over-preparedness" in the context of risk based decisions. Meanwhile, a low Type-II error probability implies that if there were a trend, there is a low chance we would conclude that a trend would not exist. Vice-versa, high type-II error probabilities imply that if there were a trend, there is a high chance we would conclude that a trend will not exist, which is associated with "under-preparedness". Hecht (2016) identified sites with trends within the 5% significance level based on Type-I error probabilities (standard hypothesis test with H_0: no trend). Similarly, we consider sites or clusters to have significant trends within the 5% significance level based on Type-I error probabilities. Shown in Figure 4 is the decision matrix of NHST.

	No Trend	Trend
No Action	$1 - \alpha$	β, Type II Error (Under-preparedness)
Action	α, Type I Error (Over-preparedness)	$1 - \beta$

Figure 4. NHST decision matrix

The second NHST test, MK test, is a nonparametric trend test and goes through a rank-based method as opposed to the linear regression method of the NHST. The MK test statistic, S

$$S = \sum_{i=1}^{n-1} \sum_{j=i+1}^{n} sign(x_i - x_j) \tag{12}$$

where x is the annual maximum peak 3-s gust wind data series. If $x_i > x_j$, $\text{sign}(x_i - x_j)$ is equal to +1; else, if $x_i < x_j$, $\text{sign}(x_i - x_j)$ is equal to -1. Furthermore, for independent and identically distributed (ie. iid) random variables

$$E(S) = 0 \tag{13}$$

$$Var(S) = \sigma^2 = \frac{n(n-1)(2n+5)}{18} \tag{14}$$

where n is the length of annual maximum peak 3-s gust wind data series. When $n > 10$,

$$Z_s = \begin{cases} \dfrac{S-1}{\sigma} \; for \; S > 0 \\ \dfrac{S+1}{\sigma} \; for \; S < 0 \\ 0 \; for \; S = 0 \end{cases} \tag{15}$$

the test statistic follows a normal distribution (Kendall 1962). With Z_s, the significance value (ie. p-value) of the MK test can be obtained via

$$p = 2[1 - \Phi(|Z_s|)] \tag{16}$$

where $\Phi(|Z_s|)$ is the cumulative distribution function of a standard normal distribution of Z_s. Similar to the Student's t-test, we consider sites or clusters to have significant trends within the 5% significance level based on p.

Wind Station Characterization

As it was previously mentioned, sites in this study follow these requirements: a) at least 18 years of annual data (5 years for tropical storms) and b) pre-whitened time series following von Storch (1999) if lag-1 autocorrelation is within 5% significance level. Figure 5 is a map of the sites by type of storms considered for the study, where sites that show significant positive trends using the MK tests are identified with a red triangle. Sites that do not exhibit a significant trend are shown with a black dot, and those with significant negative trends are shown as a blue

triangle. From Figure 5 in the commingled data, 17 stations (16%) show significant positive trends, evenly distributed from Florida to Massachusetts. Six stations (6%) in New England show significant negative trends. For non-thunderstorms data, 25 stations (23%) show significant positive trends, also evenly distributed from Florida to Massachusetts. Six stations (6%) in New England also show significant negative trends. For thunderstorms, 17 stations (12%) show significant positive trends, mostly distributed in Florida and some in Massachusetts. Two stations (2%) each in Florida and Maine show significant negative trends. For tropical storms, six stations (5%) show significant positive trends, three in Florida, two in the Baltimore-DC Metro Area and one in Massachusetts. Ten stations (8%) in show significant negative trends primarily in Florida and Massachusetts. Because of the short record length, we will not focus on the results for

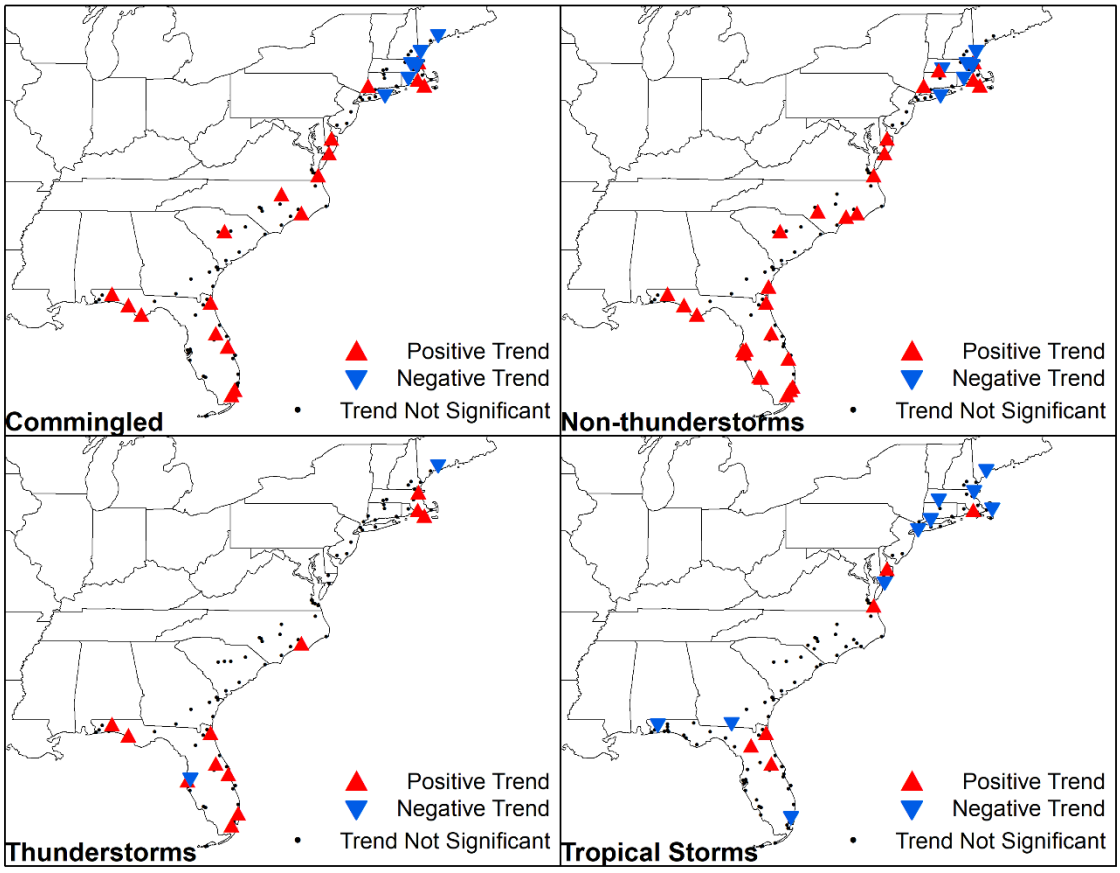

Figure 5. Stations considered in the study; trend significances based on NHST and Mann-Kendall test by storm type

tropical storms. As a result the next section will be focused on the commingled record. Results for thunderstorm and non-thunderstorm will be included in future work.

Clustering

Cluster analyses are often used in climate studies to define areas with alike climatological characteristics. Among several analyses methods, *k*-means clustering is the most widely used clustering method on extreme wind studies (Kruger et al., 2012; Blender et al.,1997; Leckebusch et al., 2008).

k-means clustering (MacQueen 1967) is an unsupervised machine learning algorithm that aims to cluster N observations (i.e. sites) into k centroids, as it tries to minimize the within-cluster sum of squares.

First, the selection of k is imperative. Several methods to determine the optimal value of k exist, of which the most commonly used is the "rule of thumb" introduced by Mardia et al. (1979), and is defined as

$$k \approx \sqrt{n/2} \tag{17}$$

where n is the number of data points (sites).

Once the k value is selected, *k*-means clustering method follows the following algorithm:

1. Place k amount of centroids into the object space
2. Assign each data point to a cluster that has the closest centroid
3. Calculate the centroids of each cluster
4. Steps 2 and 3 are reiterated until the objective function can be improved no more (i.e. global minimum achieved)

The objective function is

$$arg\min_{c}\sum_{i=1}^{k}\sum_{x\in c_i} d(x,\mu_i) \tag{18}$$

where c_i is the set of data points in cluster i and $d(x,\mu_i)$ is the Euclidean distance between a certain data point and the centroid of cluster i.

Shown in Table 1 are the variables that were considered for the clustering analysis.

Table 1. Variables used for clustering analysis of extreme winds in Eastern Seaboard

Physical variables	**Wind variables**
Latitude	Coefficient of variation C_v
Longitude	L-CV τ_2
Elevation	L-Skewness τ_3
Distance to water d	L-Kurtosis τ_4
Angle of distance to water ϕ	Average wind direction

As it was mentioned that Hong and Ye (2014) suggests the use of the latitude, longitude and L-CV for the clustering of extreme winds, this will be taken into as one of the variable combinations. Therefore, since clustering will be based on L-moment variables, L-moment variables need to be normalized prior to clustering. The standardized rth order L-moment at site i is:

$$\lambda'_{i,r} = \frac{\lambda_{i,r}}{\lambda_{i,1}} = \frac{\lambda_{i,r}}{\mu_{i,1}} \tag{19}$$

where $\lambda_{i,r}$ is the rth order L-moment at site i and $\lambda_{i,1}$ is the 1st order L-moment of at site i (the 1st order L-moment is also the arithmetic mean). With the new standardized L-moment values, higher order L-moment values τ_n are also therefore standardized using equation (6).

In addition, other variables in Table 1 aside from the L-moments also vary widely. Since clustering methods are very sensitive to range differences (Mardia et al., 1980), variables are normalized using the Z-Score normalization (Mohamad and Usman, 2013). The Z-score normalization is widely used (Parajka et al., 2010; Marzban and Sandgathe 2006; Puvaneswaran

1990) and makes the variable have a mean of 0 and standard deviation of 1 prior to cluster analysis. The Z-score normalization formula is as follows:

$$x' = \frac{x - \mu_x}{\sigma_x} \tag{20}$$

where x' is the normalized value, x is the original value, μ_x is the mean of x and σ_x is the standard deviation of x.

A technique that is used for measuring the quality of clustering is silhouette (Rousseeuw 1987). The silhouette formula is defined as

$$s(i) = \frac{b(i) - a(i)}{max\{a(i), b(i)\}} \tag{21}$$

where a is the average distance to all other data points from data point i in a cluster, and b is the minimum average distance from data point i in a cluster to all points in another cluster. We use silhouette widths to determine the optimal combination of three variables after *k*-means clustering.

Homogeneity and Heterogeneity

When clusters are formed, one must also check for the homogeneity and heterogeneity of the clusters. This is to see how homogeneous or heterogeneous the cluster is and to identify if there are any dissimilar observations (ie. sites) within the cluster.

The discordancy measure, D_i, was introduced by Hosking and Wallis (1997) to indicate if a certain site i is deemed as unusual from the cluster (i.e. site i that have significantly different sample L-moments from others within the cluster). Sites that are discordant within a cluster are disregarded due to inconsistency or gross errors. D_i is defined as

$$D_i = \frac{1}{3}(u_i - \bar{u})^T S^{-1}(u_i - \bar{u}) \tag{22}$$

where $u_i = [\tau_{2,i} \quad \tau_{3,i} \quad \tau_{4,i}]$;

Table 2. Discordancy measure critical values based on number of sites

Number of sites	Critical value
5	1.333
6	1.648
7	1.917
8	2.140
9	2.329
10	2.491
11	2.632
12	2.757
13	2.869
14	2.971
≥ 15	3

$$S = (N_S - 1)^{-1} \sum_{i=1}^{N_S} (u_i - \bar{u})(u_i - \bar{u})^T \tag{23}$$

$$\bar{u} = N_S^{-1} \sum_{i=1}^{N_S} u_i \tag{24}$$

where N_S is the number of sites in the cluster. Such a site is deemed as discordant if its D_i is above the critical value shown in Table 2. Removing discordant sites improve homogeneity of the cluster.

After discordant sites are removed from every cluster, we assess homogeneity for every processed cluster using the heterogeneity measure H_1:

$$H_1 = \frac{V_1 - \mu_V}{\sigma_V} \tag{25}$$

and V_1, dispersion measure of L-CV, is given as

$$V_1 = \left\{ \sum_{i=1}^{N_S} N_i \left(\tau_2^{(i)} - \tau_2 \right)^2 \Big/ \sum_{i=1}^{N_S} N_i \right\}^{1/2} \tag{26}$$

where N_S is the number of sites, N_i is the data length at each station and $\bar{\tau}_2$ is the mean of $\tau_2^{(i)}$, which is given as

$$\tau_2^{(i)} = \left(\sum_{i=1}^{N_S} N_i \tau_2^{(i)} \right) \Big/ \sum_{i=1}^{N_S} N_i \tag{27}$$

Generally, heterogeneity measure is defined as H_i for $i = 1,2,3$. However, Hosking and Wallis (1997) state that the H_1 statistic is practically sufficient for heterogeneity measure. H_2 and H_3 statistics lack the power of discriminating between homogeneous and heterogeneous regions because they do not yield $H_i > 2$ often. Lu (1992) showed similar results from flood frequency investigations. Therefore, H_1 based on V_1 statistic is solely used as a principal indicator of heterogeneity in this study.

Nonstationary Analysis

While clustered regions are assumed to have equivalent frequency distributions, site estimates within a region could be different. Therefore, we also incorporate the use of the index procedure as part of regional frequency analysis on extreme winds as demonstrated from Hong and Ye (2014). In the field of hydrology, the index method (Dalrymple 1960) is a commonly used method for pooling flood data series. This method has also been applied to other types of phenomena such as wave heights (Ma et al., 2006), precipitation (Onibon et al., 2004), earthquakes (Thompson et al., 2007) and extreme winds (Hong and Ye 2014). Similar to Hong and Ye (2014), we apply the index methodology to the annual maximum peak 3-s gust wind time series. Once regions were clustered, we assume that the indexed annual maximum 3-s gust wind

data within a region have an equivalent frequency distribution. We obtain the n-year return level of annual maximum peak 3-s gust wind time series at site i, $V_{c,i}$, which is given by

$$V_{c,i}(n) = v_c(n)\overline{v_{c,i}} \tag{28}$$

where v'_c is the n-year return level of annual maximum peak the cluster c and $\overline{v_{c,i}}$ is the scaling factor which is the mean value of the annual maximum peak 3-s gust wind time series from site i within cluster c. The newly obtained V, which is $V_{c,i}$, is now used in (8) instead of v in order to test for nonstationarity behavior on return levels.

To test for nonstationarity behavior on return levels, we follow a postulate that the simple regression model in (8) is used to derive conditional moments needed to convert the stationary probability distributions to describe their nonstationary counterparts (Serago and Vogel 2018). Vogel et al. (2011) and Prosdocimi et al. (2014) examined flood trends for rivers in the US and UK with the simple regression model in (8) with t. The regression model of (8) is rewritten as:

$$y_t = \mu_y + \beta(w - \mu_t) + \varepsilon \tag{29}$$

where y_t is an explanatory variable y that depends upon the explanatory variables t, μ_y is the mean of y and μ_t is the mean of t. β is the linear regression coefficient and ε represents the model error term, which is assumed to be independent with time and to have zero mean and to be heteroskedastic (i.e. constant variance) with

$$\sigma_\varepsilon^2 = (1 - \rho^2)\sigma_y^2 = \sigma_y^2 - \hat{\beta}^2\sigma_t^2 \tag{30}$$

where ρ is denoted as the cross-correlation coefficient between y and t, which is defined as $\beta = \rho\sigma_y/\sigma_t$. Sample estimate of the regression coefficient in (29) is defined as:

$$\hat{\beta} = \hat{\rho}\frac{s_y}{s_t} \tag{31}$$

where $s_y = \sqrt{\frac{1}{n-1}\sum_{i=1}^{n}(y_i - \bar{y})^2}$, $s_w = \sqrt{\frac{1}{n-1}\sum_{i=1}^{n}(w_i - \bar{w})^2}$, $\bar{y} = \frac{1}{n}\sum_{i=1}^{n} y_i$ and $\bar{t} = \frac{1}{n}\sum_{i=1}^{n} t_i$.

The expectation of (29) leads to an expression for the mean of y, condition upon t:

$$\mu_{y|t} = \mu_y + \beta(t - \mu_t) \tag{32}$$

Similarly, the variance of y, conditioned upon t, is obtained by taking the variance of (29):

$$\sigma^2_{y|t} = \sigma^2_\varepsilon = \sigma^2_y(1 - \rho^2) \tag{33}$$

Nonstationarity in a LN2 Probability Distribution

Finally, we demonstrate how the behavior of the return levels of annual maximum peak 3-s gust wind data fluctuate depending on a nonstationary trend. While several extreme value probability distributions, such as extreme value distributions, log-Pearson III distribution and 3-parameter lognormal distribution, are more widely used for extreme scenarios, we use a simple, realistic and representative two-parameter lognormal distribution (LN2) model for our study (Read and Vogel, 2015). As it was shown in Figure 3, annual maximum peak 3-s gust wind data are well fit by the LN2 distribution as compared to other distributions. Studies involving annual maximum phenomena have provided parsimonious procedures with the LN2 and have been commonly applied for annual maximum flood studies (Stedinger and Crainiceanu, 2000). We hypothesize that this equivalent procedure is applicable for the annual maximum peak 3-s gust wind data series by using previously derived nonstationary LN2 models (Vogel et al., 2011; Hecht, 2016; Serago and Vogel 2018).

The two-parameter lognormal distribution (LN2), or typically known as lognormal distribution, is one of the most widely used distributions in describing natural phenomena. Stedinger (1980) provided quantile estimation methods for the LN2 via maximum likelihood estimators. The following is a quantile function of a stationary LN2:

$$\hat{x}_{p,STA} = \exp\left(\bar{y} + z_p s_y\right) \tag{34}$$

where $\bar{y}$ is the sample mean of y, s_y is the sample standard deviation of y, and z_p is the inverse of a standard normal variable with nonexceedance probability p. Substitution of the conditional moments of y into the stationary quantile function yields the nonstationary quantile function of LN2:

$$\hat{x}_{p,NSTA} = \exp\left(\hat{\mu}_{y|t} + z_p \hat{\sigma}_{y|t}\right) = \exp\left(\bar{y} + \hat{\beta}(t_i - \bar{t}) + z_p \sqrt{s_y^2 - \hat{\beta}^2 s_t^2}\right) \tag{35}$$

where $\hat{\beta}$ is the regression coefficient obtained in (31), t_i are a series of explanatory variables (i.e. time), $\bar{t}$ is the sample mean of t and s_t is the sample standard deviation of t. Note that when $\hat{\beta} = 0$ for the nonstationary quantile function, it yields the stationary quantile function.

To model nonstationarity, this study adopts the homoscedastic model, one of the nonstationary regression models introduced by Hecht (2016). The homoscedastic model uses the equivalent quantile function in (35). Trends applied onto the log-space mean correspond to a concurrent trend in the real-space variance that enables the real-space coefficient of variation to remain unchanged. Similarly, trends applied to the log-space variance relate to trends in the real-space coefficient of variance. Coefficient of variance is a distinct indicator of change in relative variability compared to the mean, and would normalize changes in the absolute real-space variance so it would have concurrent changes in the real-space mean.

The homoscedastic nonstationary LN2, is a regression model that produces annual maximum series with LN2 distribution with a time-conditional mean. The time dependent expectation of Y is:

$$E[Y(t)] = \mu_{y|t_n} = \beta_0 + \beta_1 t_n \tag{36}$$

where t_n is the particular response variable (time) of interest. The model is assumed to have an error of a mean of zero, constant variance (i.e. homoscedastic), serially independent and

approximately normally distributed. As such, the conditional variance of Y at time t_n is similar to (33), which is equivalent to:

$$Var[Y|t_n] = \sigma^2_{y|t_n} = \sigma^2_{\varepsilon} = \sigma^2_y - \beta_1^2\sigma_t^2 \tag{37}$$

Using (36) and (37), the homoscedastic nonstationary model quantile function can be derived:

$$\hat{x}_{NSTA} = \exp\left(\hat{\mu}_{y|w} + z_p\hat{\sigma}_{y|w}\right) = \exp\left(\beta_0 + \beta_1 t_n + z_p\sqrt{\sigma_y^2 - \beta_1^2\sigma_t^2}\right) \tag{38}$$

As a whole, Figure 6 shows the methodology of this study**.**

Results & Analysis

It has been shown in Figure 5 that several stations exhibit nonstationarity by storm type. In this study, we considered a station, Jacksonville Executive at Craig Airport, to see nonstationarity at a single station by storm type. Jacksonville Executive at Craig Airport shows nonstationarity for annual maximum peak 3-s gust wind data series for all four types of storms (commingled, non-thunderstorms, thunderstorms and tropical storms). Regression plots for each storm type in Jacksonville Executive at Craig Airport (KCRG) are shown in Figure 2. Figure 2 uses circles to show the $y = \ln(v)$, where v is annual maximum peak 3-s gust wind data series and t (time) relationship. Shown in Figure 2 is also the goodness-of-fit metric R^2, sample size n, attained significance level q and the P-value of a nonparametric trend test (MK test) p. As

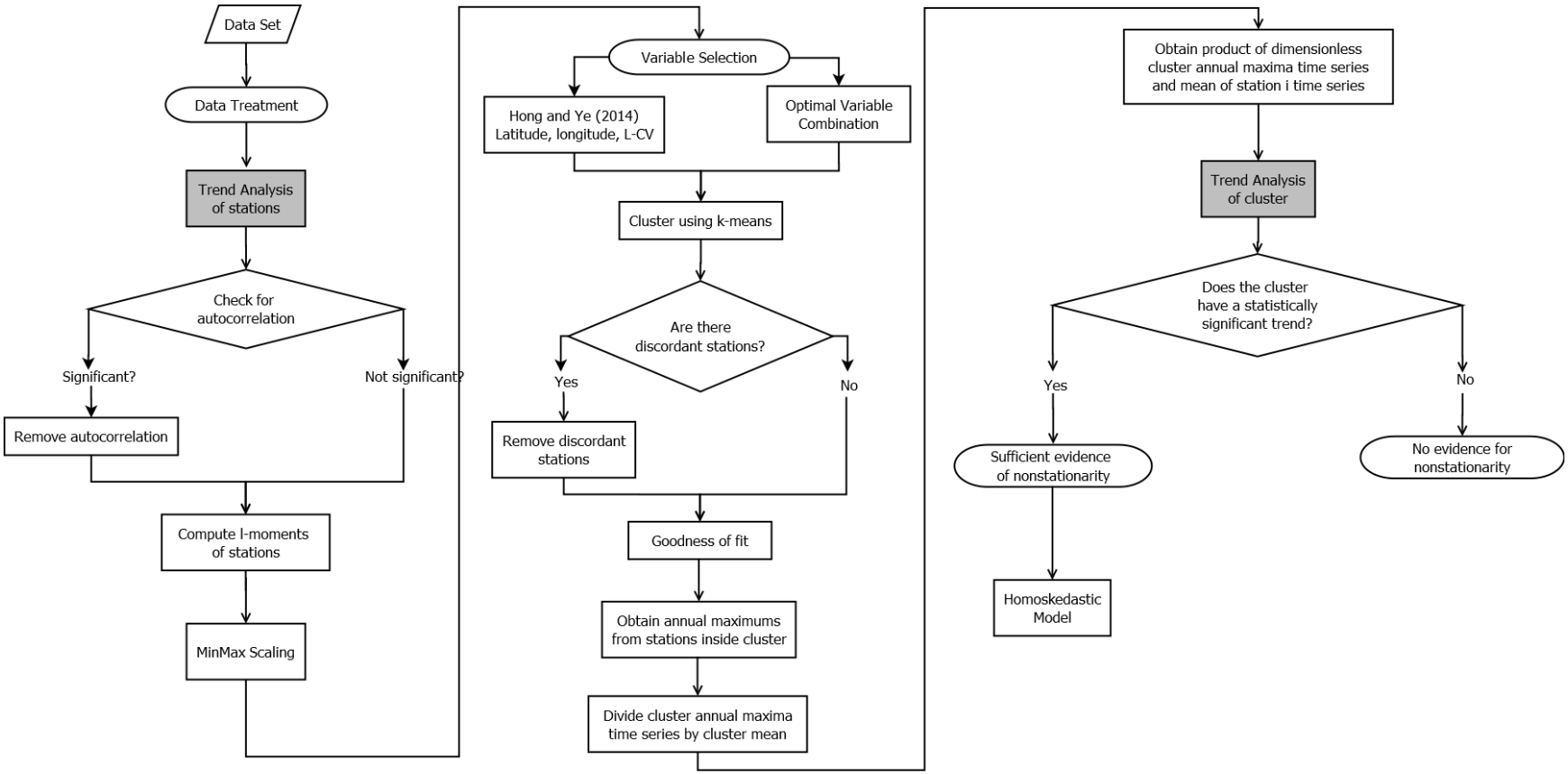

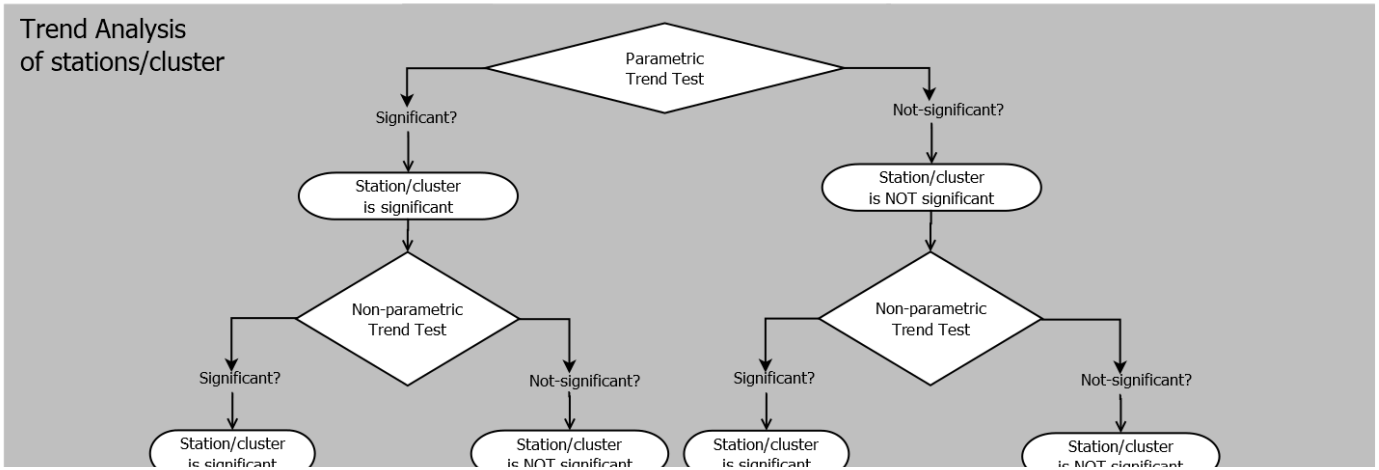

Figure 6. Methodology Flowchart

mentioned before, it is seen that all storm types from KCRG show significant trends based on the nonparametric trend test. For attained significance level, q, it is seen that commingled and thunderstorm storm types show extremely low values. As shown from a similar study from Serago and Vogel (2018), this can be interpreted as proof that a trend is so strong that there is little possibility for evidence for a trend as strong as or stronger to happen if there were no trend. The significant statistics by station are shown in Table A.5-8 by storm type in the appendix.

Based on the methodology presented before, *k*-means clustering is done for the 108 sites. However, selection of *k* is required before the cluster analysis. By using (17), a heuristic method of calculating *k* (Mardia et al., 1980), a *k* value of 7.35 is obtained. However, since *k* value needs to be an integer greater than 0, the nearest integer 7 is used as *k* value for the *k*-means clustering.

Shown in Table 3 are the clustered statistics on the Eastern Seaboard based on the variable combination of latitude, longitude, and L-CV as suggested by Hong and Ye (2014) and the commingled time series. Figure 7 show spatial distribution of the identified clusters on the Eastern Seaboard via the Hong and Ye combination. The figure has colored dots, representing wind recording sites that belong to a certain cluster. Encircled colored dots represent a wind recording station that belongs to a certain cluster but is regarded discordant within the cluster and has been removed from the analysis.

The Hong and Ye clusters have five acceptably homogeneous clusters, one possibly heterogeneous cluster and one definitely heterogeneous cluster. One of the homogeneous clusters from the Hong and Ye combination, cluster 6, has a discordant station. This discordant station is Westover Afb/Metropolitan Airport in Massachusetts. The discordancy index for this station was approximately 3.0143, a value very close to the critical value, 3.00. We hypothesize the discordancy of this station to be because it is one of the stations that is the furthest away from the

Table 3. Cluster Analysis Statistics (Latitude, Longitude and L-CV) for commingled time series

N_{cl}	ID	N_s	N_d	H	$\hat{\beta}_1$	α	p	TH
7	1	23	0	3.874	0.001	0.297	0.762	DHet
	2	19	0	-1.751	0.007	0.000	0.001	AHom
	3	3	0	-0.289	0.005	0.166	0.252	AHom
	4	9	0	-1.899	0.007	0.002	0.014	AHom
	5	14	0	0.975	0.004	0.015	0.047	AHom
	6	20	1	0.238	-0.002	0.905	0.139	AHom
	7	20	0	1.791	0.003	0.004	0.016	PHet

Note: N_{cl} = Number of clusters; ID = Cluster ID; N_s = Number of sites within a cluster; N_d = Number of discordant sites within a cluster; TH = Type of region; AHom = acceptably homogeneous; PHet = possibly heterogeneous; DHet = definitely heterogeneous; for H, α, p and $\hat{\beta}_1$ see (11), (19), (26) and (31)

coast. Cluster 2, 4, 5 and 7 are homogeneous clusters and show significant trends.

However, since cluster 7 is heterogeneous, only clusters 2, 4, and 5 will be further analyzed in this study.

Figures 8 show the clusters' and sites' trend coefficients and significances based on the Hong and Ye. Clusters that are significant have a white background; otherwise, clusters are have

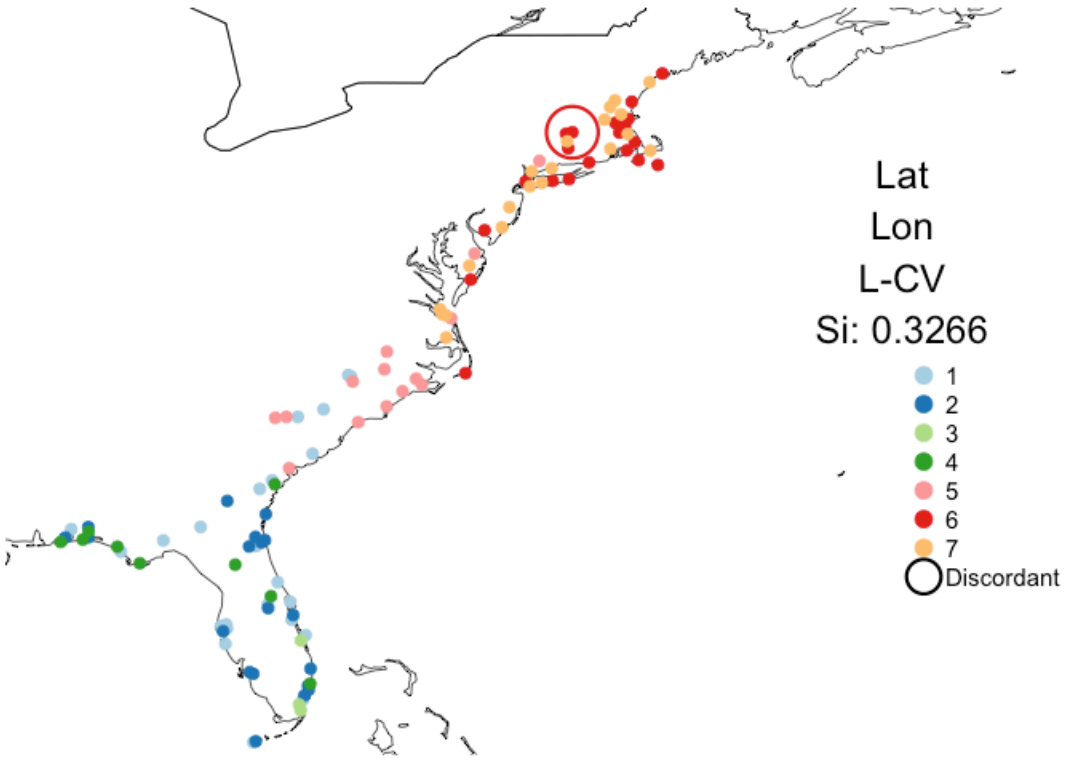

Figure 7. Clustering Distribution of Hong and Ye Combination as Variables

a gray background. From these results, it is apparent that sites in Florida until the Carolinas as represented by the homogeneous clusters 2, 4 and 5 show the most significant nonstationarity. Cluster 2 and 4 from the Hong and Ye combinations sites from Florida, and cluster 5 mostly depicts sites from the Carolinas.

Regression plots for the clusters used in the study, 2, 4 and 5 are shown in Figures 9, 10 and 11, respectively. We now use the nonstationary homoscedastic trend model (38) to estimate return levels of peak 3-s gust wind for each sites of each cluster. Shown in Figures 12, 13 and 14 are comparisons of the return levels of peak 3-s gust wind for the commingled time series on a stationary model vs a nonstationary homoscedastic model for clusters 2, 4 and 5 via Hong and Ye combination. Return levels are computed for 100, 300, 700 and 1700 year events and three time of interests were used: 2010, 2030, and 2050. It is seen from Figures 12, 13 and 14 that for

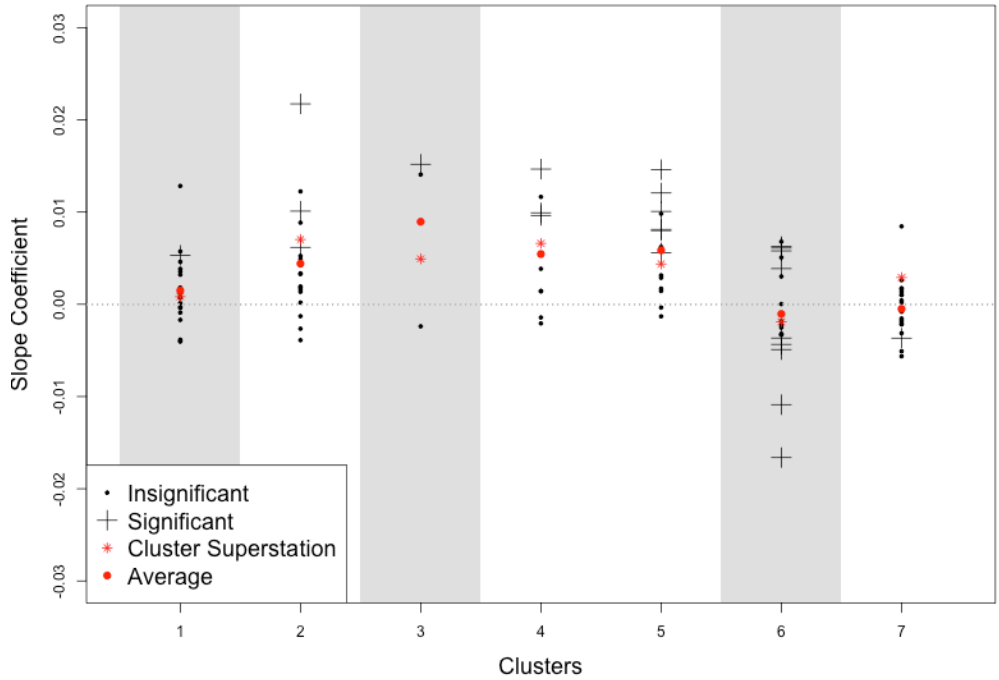

Figure 8. Slope Analysis by Clusters from 7-means via Hong and Ye combination

all return levels from 7-means via Hong and Ye combination show increase with the time of interest due to the significant positive slope.

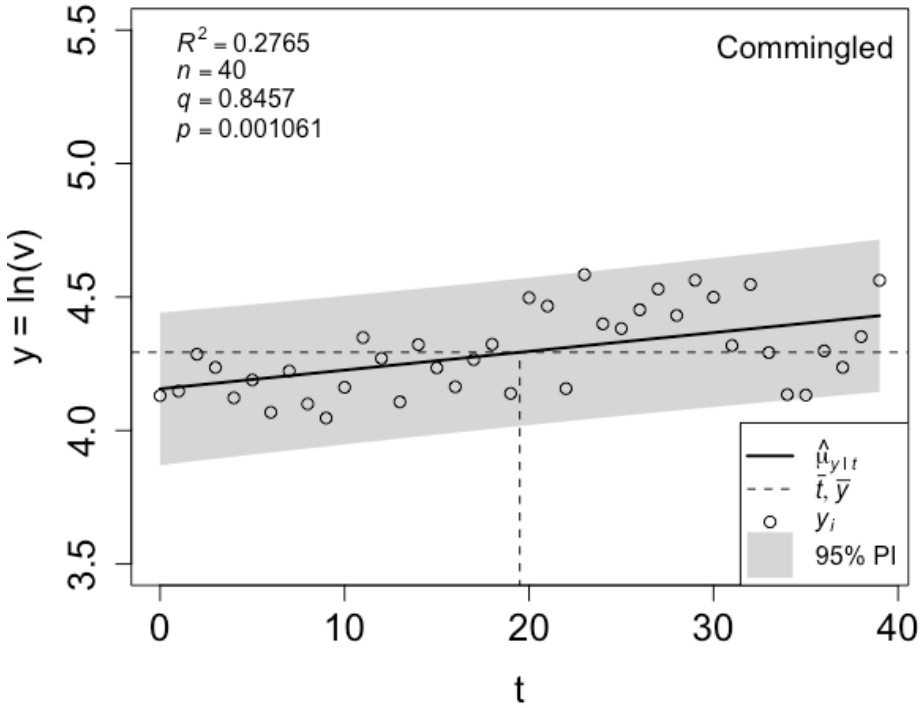

Figure 9. Regression Plot of Cluster 2 from 7-means via Hong and Ye Combination; solid black line represents regression line, gray shade represents 95% prediction interval and dashed line represents conditional means of y and t

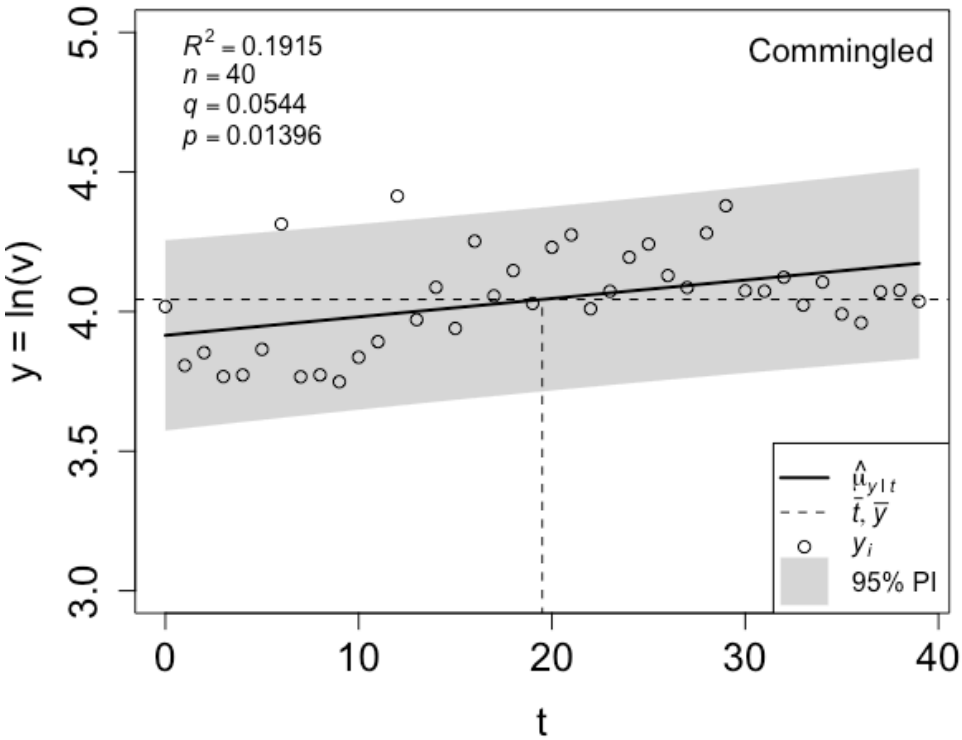

Figure 10. Regression Plot of Cluster 4 from 7-means via Hong and Ye Combination; solid black line represents regression line, gray shade represents 95% prediction interval and dashed line represents conditional means of y and t

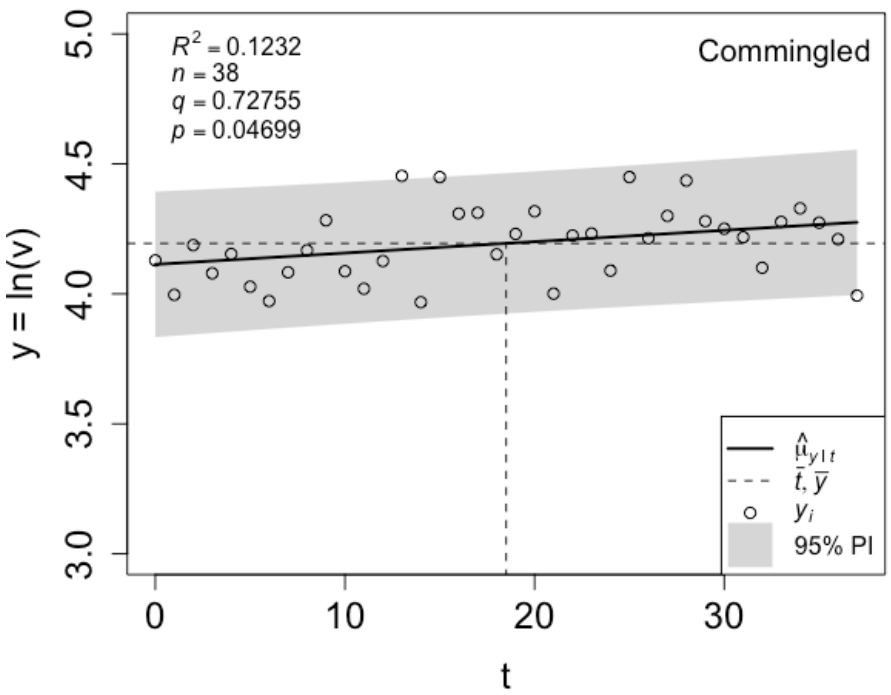

Figure 11. Regression Plot of Cluster 5 from 7-means via Hong and Ye Combination; solid black line represents regression line, gray shade represents 95% prediction interval and dashed line represents conditional means of y and t

We can infer that when homoscedastic trend is applied, the return level of peak 3-s gust wind increases drastically for all return periods. Some particular sites (16 and 18) in Cluster 1 via the Hong and Ye combination show the highest return levels from all sites within the cluster. These sites are located on the southwestern region coast in Florida and share a common characteristic that they are near the Gulf of Mexico. Some sites (5, 6 and 7) in cluster 2 also show the same phenomena by having high return level periods compared to other sites. These results are consistent with the positive correlation findings between SST (sea surface temperature) and Gulf of Mexico wind speeds predicted by Trepanier (2013), and the theory of maximum potential intensity in tropical storms studied by Emanuel (1986).

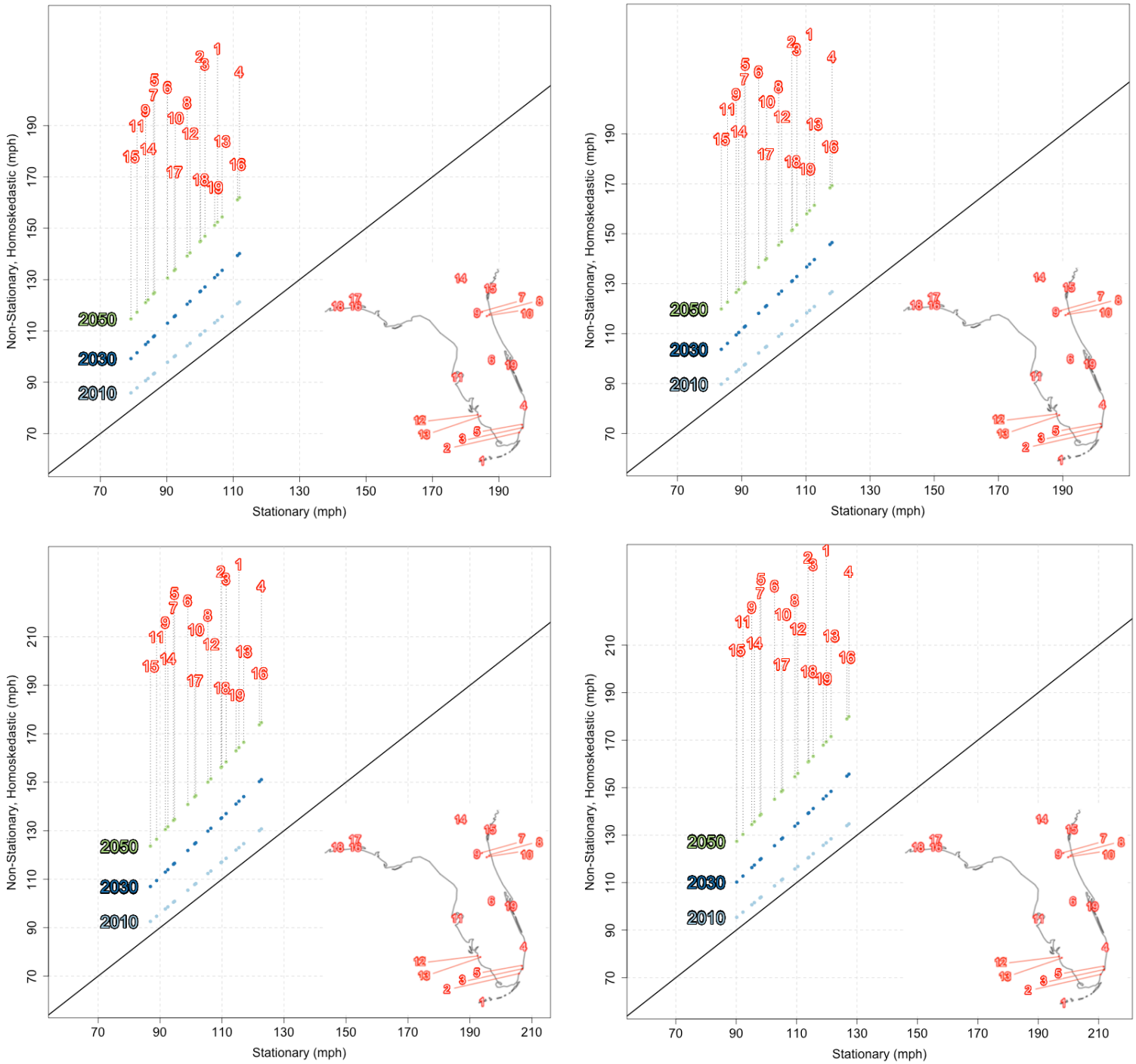

Figure 12. Return level (100, 300, 700, 1700 year) comparison of stationary and nonstationary trends (cluster 2 from 7-means via Hong and Ye combination); light blue, blue and light green poin indicate return level data points; black solid line is a 1:1 line

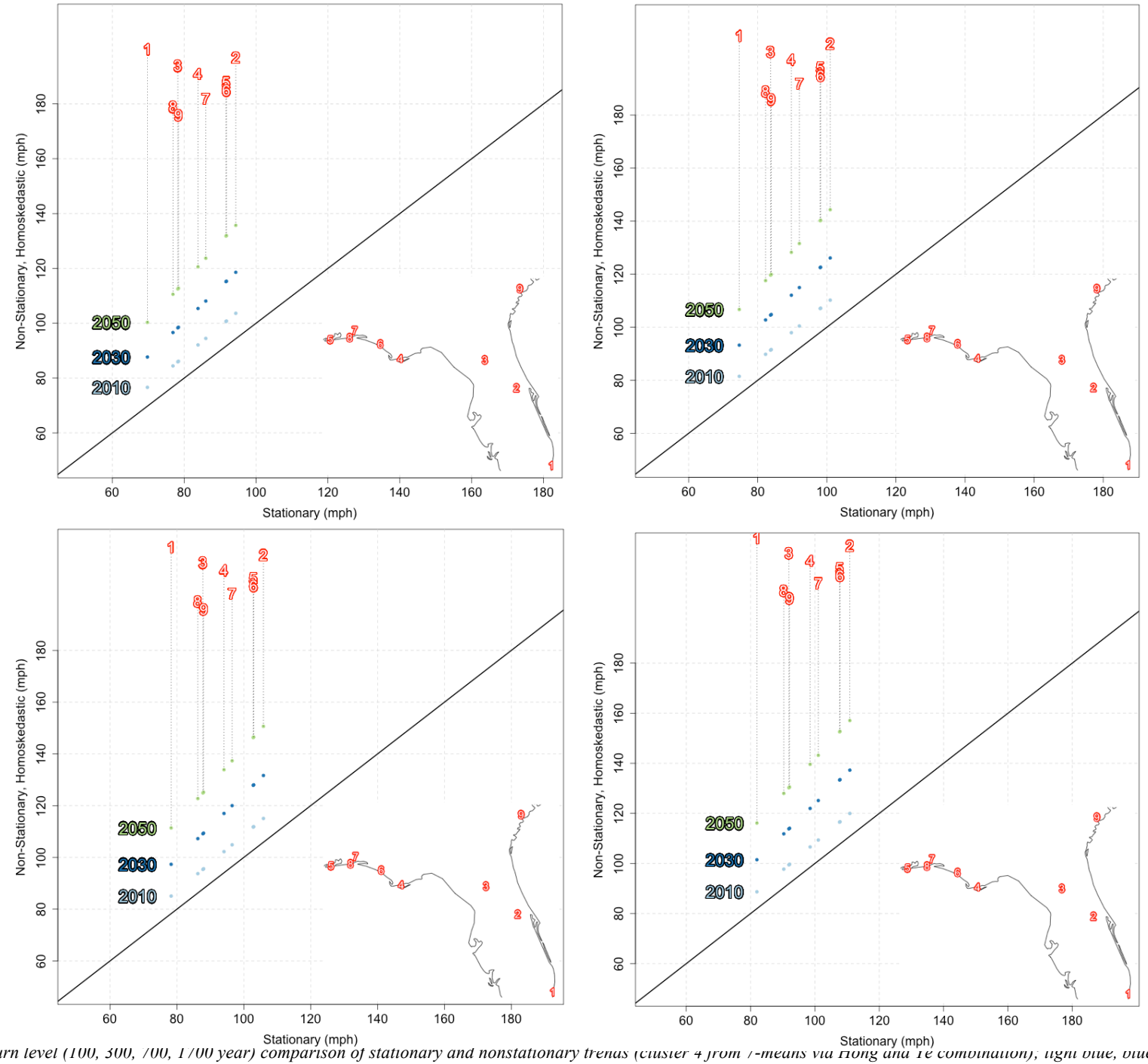

Figure 13. Return level (100, 300, 700, 1700 year) comparison of stationary and nonstationary trends (cluster 4 from 7-means via Hong and Ye combination); light blue, blue and light green poin indicate return level data points; black solid line is a 1:1 line

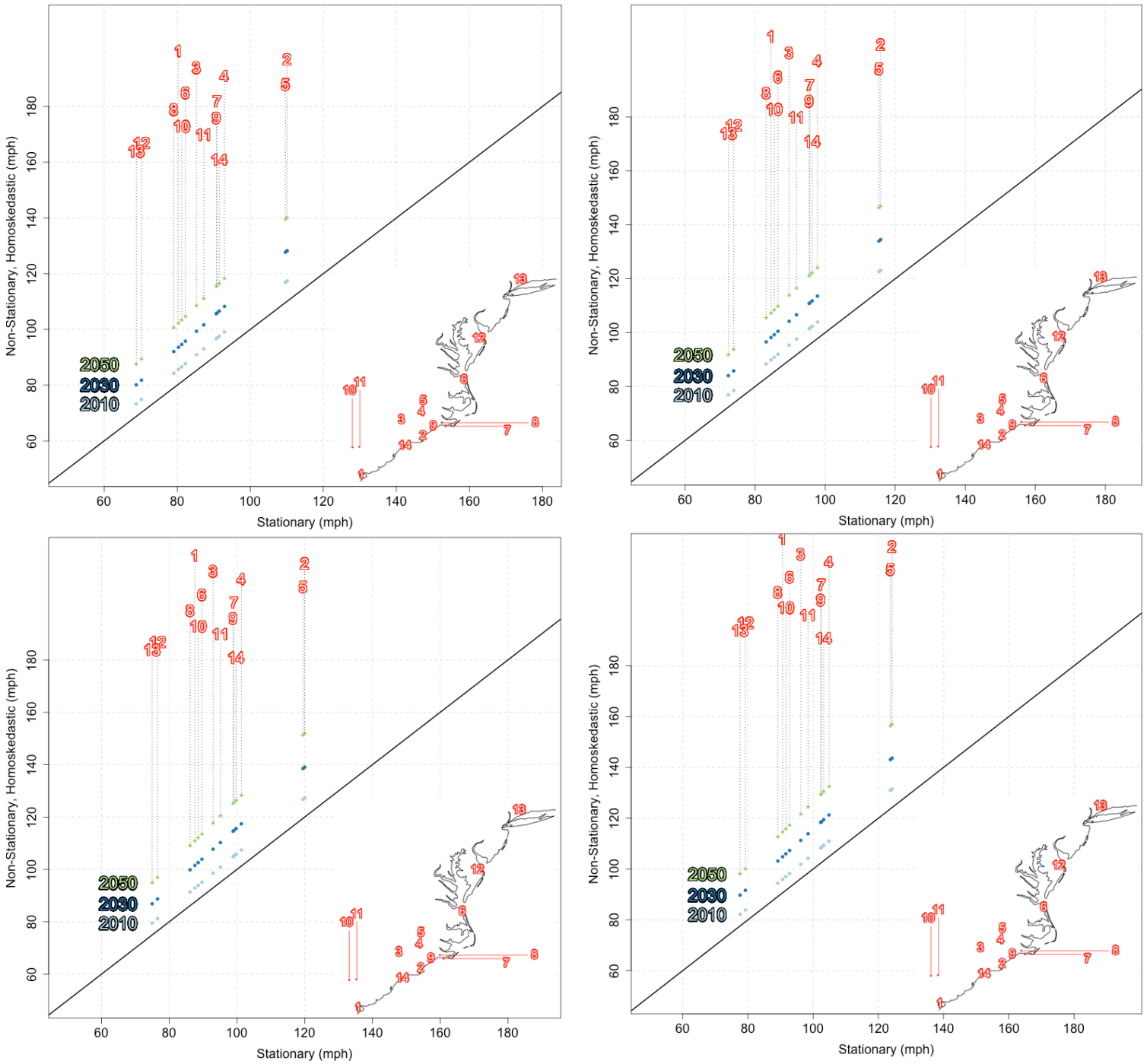

Figure 14. Return level (100, 300, 700, 1700 year) comparison of stationary and nonstationary trends (cluster 5 from 7-means via Hong and Ye combination); light blue, blue and light green poin indicate return level data points; black solid line is a 1:1 line

Discussion

As shown from Figure 7, clusters 1 to 4 for Hong and Ye combination are composed of clusters in the Florida region. Clusters 5-7 represent regions from the Carolinas through New England. It can also be seen from Table 3 that cluster 2 and 4 have relatively lower a and p compared to other clusters from the Hong and Ye combination representing the most significant trend. This is because magnitude of trends, $\hat{\beta}_1$, are higher as seen from Table 3 or Figure 8. Furthermore, clusters 2-6 show more homogeneity (ie. negative H compared to clusters 1 and 7).

Meanwhile, clusters 5-7 show lower values of $\hat{\beta}_1$. In addition, while cluster 5 and 6 are homogeneous, their H values are generally higher compared to the Florida region with the exception of cluster 1. We find these high values of H to be an irregularity; however, it is seen from Figure 17 that the majority of major hurricanes that land from the Carolinas to the New England area dissipate shortly after landfall. Whereas in the Florida region, most of the hurricanes cross the peninsula. From these hurricane tracks, we can infer that sites nearby the coast in the Carolinas to the New England area could possibly have different characteristics that the coastal storms. This may have impacted the formation of cluster 6 and 7.

Conclusion

In this study, we have evaluated the observational record of annual maximum 3-s wind gust on both individual stations and regional clusters along the Eastern Seaboard. For the cluster analysis, a variety of physical (eg. Latitude/longitude coordinates) and wind characteristic (ie. L-moments of annual maximum peak 3-s gust wind) variables have been considered as shown in Table 1. An index method was incorporated which allowed for the site mean to change with an assumption that the frequency distribution were equivalent for all sites within a cluster. The cluster analysis recommended by Hong and Ye (2014) (latitude, longitude and L-CV) was used. As seen from Table 3 (Figure 7), the Hong and Ye combination has identified 5 homogeneous clusters and three with significant nonstationary trends. With sites in the Eastern Seaboard clustered, stationary and a LN2 nonstationary homoscedastic models were used to compute return levels.

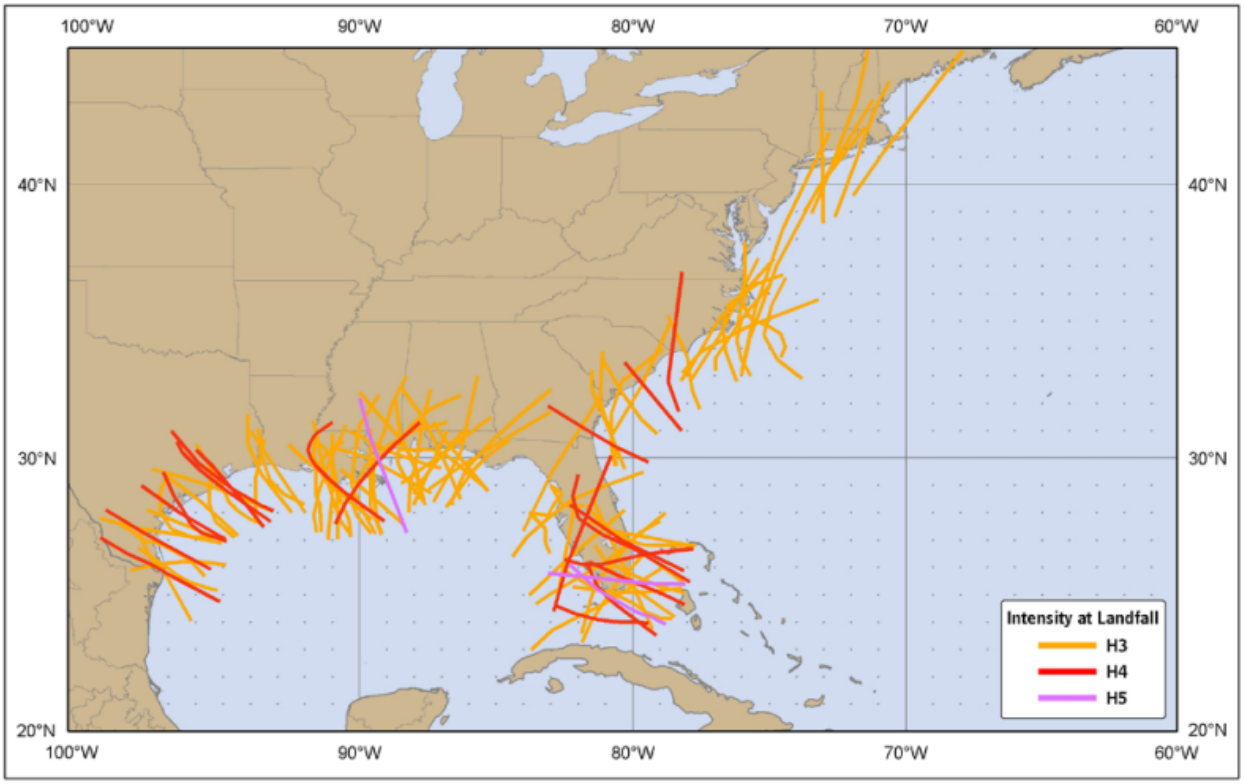

Figure 15. United States major hurricane strikes (category 3 or higher), 1851-2010. (from Blake et al, 2011)

The extreme wind data used in this study were divided by storm types (commingled, nonthunderstorms, thunderstorms and tropical storms) and evidence of nonstationarity by storm types were observed. For commingled data, 23 out of 108 stations exhibit evidence of nonstationarity. 16% of these stations show positive trends and 6% show negative trends. For nonthunderstorm data, 31 out of 108 stations exhibit evidence of nonstationarity. 23% of these stations show positive trends and 6% show negative trends. For thunderstorm data, 19 out of 99 stations exhibit evidence of nonstationarity. 19% of these stations show positive trends and 2% show negative trends. For tropical storm data, 16 out of 117 stations exhibit evidence of nonstationarity. 5% of these stations show positive trends and 8% show negative trends.

Once regional frequency analysis and *k*-means clustering were applied, we were able to find nonstationarity of the mean for regions in the Southern part of the Eastern Seaboard. Nonstationarity behavior was most significant and homogenous in the Gulf of Mexico/Florida region and into southern Georgia. Regions in the mid-Coast from the Carolinas to Baltimore-DC Metro Area also showed some significant trends. However, Baltimore-DC Metro Area to the north until New England did not show significant trends for individual sites. This has led to a formation of distinct clusters of insignificant trends compared to those in Baltimore-DC Metro Area and below. The New England region also showed negligible trends and the regional clusters were less homogeneous (less likely to cluster spatially). Furthermore, the nonstationary trend showed an increase in the mean behavior leading to higher return levels of peak 3-s gust wind under nonstationary conditions than stationary conditions.

When looking at individual stations and by storm type, 16% of stations exhibit statistically significant positive trends for commingled wind, 23% for non-thundestorms, 17% for thunderstorms, and 6% for tropical storms. An example is shown with the KCRG station,

located in Florida, which has shown significant positive trends for all types of storm type. If instead we look for nonstationarity regionally using cluster analysis the nonstationarity is focused in the southern region. The regional cluster analysis provides observational evidence that nonstationarity of wind in terms of the 3-s wind gust is not observed for from the Baltimore/DC Metro Region to New England along the Eastern Seaboard. However, a positive statistically significant trend is observed in the annual maximum of the 3-s wind gust in the regional clusters from Florida to the Carolinas. This study therefore provides observational evidence of a positive trend in regional extreme winds in the Southern region of the Eastern Seaboard. This trend can be accounted for by using a nonstationary homoscedastic model.

Appendix

Table A.1. Sites used, commingled storm data stations

Commingled								
STATION NAME	ST	CODE	LAT	LON	ELEV (m)	SIGN	MEAN	N
Key West International Airpor	FL	KEYW	24.555	-81.752	1.2	+	62.74	38
Key West Nas	FL	KNQX	24.583	-81.683	1.8	+	54.96	34
Miami International Airport	FL	KMIA	25.791	-80.316	8.8	+	61.37	38
Opa Locka Airport	FL	KOPF	25.907	-80.28	3.1	+	52.21	24
Fort Lauderdale Hol	FL	KFLL	26.072	-80.154	3.4	+	52.99	38
Homestead Afb Airport	FL	KHST	25.483	-80.383	1.5	-	39.48	27
Kendall-Tamiami Exec Arpt	FL	KTMB	25.648	-80.433	3.1	+	35.68	27
Palm Beach International Airp	FL	KPBI	26.685	-80.099	5.8	+	58.41	35
Ft Lauder Executive Arpt	FL	KFXE	26.197	-80.171	4.3	+	45.06	27
Melbourne Intl Ap	FL	KMLB	28.101	-80.644	8.2	+	59.12	37
Vero Beach Muni	FL	KVRB	27.653	-80.243	8.5	-	67.62	38
Pompano Beach Airpark Arpt	FL	KPMP	26.25	-80.108	6.4	+	35.23	22
Orlando International Airport	FL	KMCO	28.434	-81.325	27.4	+	47.11	38
Executive Airport	FL	KORL	28.545	-81.333	32.9	+	74.66	21
Daytona Beach Intl	FL	KDAB	29.183	-81.048	12.5	-	56.34	38
Orlando Sanford Airport	FL	KSFB	28.78	-81.244	16.8	+	47.64	35
Jacksonville International A	FL	KJAX	30.495	-81.694	7.9	-	44.90	38
Jacksonville Nas	FL	KNIP	30.233	-81.667	6.1	+	60.60	37
Mayport Naf	FL	KNRB	30.4	-81.417	4.9	+	50.19	32
Cecil Field Airport	FL	KVQQ	30.219	-81.876	24.7	-	43.66	27
Jacksonville/Craig	FL	KCRG	30.336	-81.515	12.5	+	48.34	37
Savannah/Hilton Head Intl Air	GA	KSAV	32.13	-81.21	14	-	57.30	34
Charleston Afb/International	SC	KCHS	32.899	-80.04	12.2	+	69.19	38
Beaufort Mcas	SC	KNBC	32.483	-80.717	11.3	+	43.53	36
Wright Aaf Airport	GA	KLHW	31.883	-81.567	13.7	-	50.93	28
St Lucie County Intl Arpt	FL	KFPR	27.498	-80.377	7.3	+	37.18	23
Albert Whitted Airport	FL	KSPG	27.765	-82.628	2.4	+	42.31	25
Page Field Airport	FL	KFMY	26.585	-81.861	4.6	+	50.65	35
Sw Florida Intn Airport	FL	KRSW	26.536	-81.755	9.5	+	55.69	27
Tampa International Airport	FL	KTPA	27.962	-82.54	5.8	-	51.45	38
Sarasota/Bradenton Intl Ap	FL	KSRQ	27.401	-82.559	8.5	+	62.63	38
St Pete-Clwtr Intl Airport	FL	KPIE	27.911	-82.688	3.4	+	50.52	38
Alma/Bacon Co.	GA	KAMG	31.536	-82.507	62.8	-	44.04	37
Malcolm Mc Kinnon Airport	GA	KSSI	31.152	-81.391	4.9	+	41.36	38
Tallahassee Regional Airport	FL	KTLH	30.393	-84.353	16.8	+	57.14	38

Gainesville Rgnl	FL	KGNV	29.692	-82.276	50.3	+	39.50	38
Valdosta Regional Airport	GA	KVLD	30.783	-83.277	60.4	-	48.66	38
Apalachicola Muni Airport	FL	KAAF	29.733	-85.033	5.8	+	42.34	33
Eglin Afb Airport	FL	KVPS	30.483	-86.517	26.5	+	58.10	36
Bob Sikes Airport	FL	KCEW	30.78	-86.523	57.9	+	48.16	38
Pensacola Regional Airport	FL	KPNS	30.478	-87.187	34.1	+	52.31	20
Pensacola Nas	FL	KNPA	30.35	-87.317	8.5	+	46.28	34
Whiting Field Naval Air Stati	FL	KNSE	30.717	-87.017	60.7	-	49.17	28
Panama City-Bay Co. Int Ap	FL	KPFN	30.212	-85.683	6.4	+	46.33	30
Eglin Af Aux Nr 3 D	FL	KEGI	30.65	-86.517	58	+	43.43	26
Wilmington Intl	NC	KILM	34.268	-77.9	11.6	+	59.65	20
Pope Afb Airport	NC	KPOB	35.174	-79.009	66.5	+	64.80	39
Fayett Rgnl/Grannis Fld Ap	NC	KFAY	34.991	-78.88	56.7	+	46.20	37
Cape Hatteras	NC	KHSE	35.233	-75.622	3.4	+	56.78	23
Seymour-Johnson Afb Airport	NC	KGSB	35.344	-77.965	33.2	+	50.36	38
Rocky Mount-Wilson Rgn Apt	NC	KRWI	35.855	-77.893	48.8	+	59.40	37
Oceana Nas	VA	KNTU	36.817	-76.033	7	+	44.56	36
Norfolk International Airport	VA	KORF	36.903	-76.192	9.1	-	80.73	38
Norfolk Nas	VA	KNGU	36.937	-76.289	5.2	+	56.11	38
Cherry Point Mcas	NC	KNKT	34.9	-76.883	8.8	+	49.25	35
Craven County Reg Airport	NC	KEWN	35.068	-77.048	5.8	-	42.82	38
Jacksonville	NC	KNCA	34.708	-77.44	7.9	+	49.14	35
Columbia Metropolitan Airport	SC	KCAE	33.942	-81.118	68.6	-	44.01	38
Mcentire Air National Guard S	SC	KMMT	33.967	-80.8	77.4	+	47.28	29
Florence Regional Airport	SC	KFLO	34.185	-79.724	44.5	+	66.80	38
Wallops Flight Facility Airpo	VA	KWAL	37.937	-75.471	14	+	49.52	25
Salisbury Ocean Cit	MD	KSBY	38.341	-75.51	18.3	-	78.67	38
Atlantic City International A	NJ	KACY	39.449	-74.567	18.3	-	60.40	38
Millville Municipal Arpt	NJ	KMIV	39.367	-75.067	21.3	-	52.94	38
Naes/Maxfield Field	NJ	KNEL	40.033	-74.35	30.8	+	60.46	30
Sussex County Airport	DE	KGED	38.689	-75.359	15.5	+	38.04	18
La Guardia Airport	NY	KLGA	40.779	-73.88	3.4	-	49.49	37
Long Island Mac Art	NY	KISP	40.794	-73.102	30.2	-	42.09	38
Westchester County Airport	NY	KHPN	41.067	-73.708	115.5	+	47.76	38
Igor I Sikorsky Memorial Airp	CT	KBDR	41.158	-73.129	1.5	-	63.12	38
Groton-New London Airport	CT	KGON	41.328	-72.049	3.1	-	46.15	38
Nantucket Mem	MA	KACK	41.253	-70.061	14.3	-	56.48	21
Plymouth Municipal Airport	MA	KPYM	41.91	-70.729	45.4	+	45.63	20
New Bedford Rgnl Airport	MA	KEWB	41.676	-70.958	24.4	+	47.01	38
Marthas Vineyard Airport	MA	KMVY	41.393	-70.615	20.7	+	52.33	38
Brnsbl Muni-Bman/Pol Fd Ap	MA	KHYA	41.669	-70.28	16.8	+	65.48	38
Theodore F Green State Airpor	RI	KPVD	41.723	-71.433	16.8	-	50.42	38
Bradley International Airport	CT	KBDL	41.938	-72.682	53.3	-	64.66	38

Danbury Municipal Airport	CT	KDXR	41.371	-73.483	139.3	+	37.26	30
Hartford-Brainard Airport	CT	KHFD	41.736	-72.651	5.8	-	47.94	36
Beverly Municipal Airport	MA	KBVY	42.584	-70.918	32.9	+	43.55	35
Gen E L Logan International A	MA	KBOS	42.361	-71.01	3.7	-	53.73	38
Naval Air Station	MA	KNZW	42.15	-70.933	49.1	-	55.85	21
Norwood Memorial Airport	MA	KOWD	42.191	-71.174	15.2	+	46.90	38
Concord Municipal Airport	NH	KCON	43.12	-71.3	105.5	+	49.94	34
Pease International Tradeport	NH	KPSM	43.083	-70.817	30.5	-	50.40	40
Portland International Jetpor	ME	KPWM	43.65	-70.3	13.7	-	58.87	38
Naval Air Station	ME	KNHZ	43.9	-69.933	21.3	-	47.68	37
Manchester Airport	NH	KMHT	42.933	-71.438	68.6	+	68.56	38
John F Kennedy International	NY	KJFK	40.639	-73.762	3.4	-	57.46	38
Republic Airport	NY	KFRG	40.734	-73.417	24.7	-	53.97	18
Francis S Gabreski Ap	NY	KFOK	40.844	-72.632	20.4	-	62.87	31
Bedford Hanscom Field	MA	KBED	42.47	-71.289	40.5	-	54.65	22
Lawrence Municipal Airport	MA	KLWM	42.717	-71.124	45.4	+	59.69	28
Fort Devens/Ayer	MA	KAYE	42.567	-71.6	82	-	49.13	18
Westover Afb/Metropolitan Air	MA	KCEF	42.2	-72.533	73.5	-	45.42	39
Barnes Municipal Airport	MA	KBAF	42.158	-72.716	82.6	+	43.97	37
Langley Afb Airport	VA	KLFI	37.083	-76.36	3.1	-	64.05	40
Simmons Aaf Airport	NC	KFBG	35.133	-78.933	74.4	+	75.27	37

Table A.2. Sites used, nonthunderstorm data stations

Non-Thunderstorms								
STATION NAME	ST	CODE	LAT	LON	ELEV (m)	SIGN	MEAN	N
Key West International Airpor	FL	KEYW	24.555	-81.752	1.2	-	40.37	38
Key West Nas	FL	KNQX	24.583	-81.683	1.8	+	45.74	34
Miami International Airport	FL	KMIA	25.791	-80.316	8.8	+	42.64	38
Opa Locka Airport	FL	KOPF	25.907	-80.28	3.1	+	45.38	24
Fort Lauderdale Hol	FL	KFLL	26.072	-80.154	3.4	-	47.05	38
Homestead Afb Airport	FL	KHST	25.483	-80.383	1.5	-	38.42	27
Kendall-Tamiami Exec Arpt	FL	KTMB	25.648	-80.433	3.1	+	34.46	27
Palm Beach International Airp	FL	KPBI	26.685	-80.099	5.8	-	43.83	35
Ft Lauder Executive Arpt	FL	KFXE	26.197	-80.171	4.3	-	37.38	27
Melbourne Intl Ap	FL	KMLB	28.101	-80.644	8.2	+	43.27	37
Vero Beach Muni	FL	KVRB	27.653	-80.243	8.5	+	56.66	38
Pompano Beach Airpark Arpt	FL	KPMP	26.25	-80.108	6.4	+	36.35	22
Orlando International Airport	FL	KMCO	28.434	-81.325	27.4	+	45.45	38
Executive Airport	FL	KORL	28.545	-81.333	32.9	+	55.94	21
Daytona Beach Intl	FL	KDAB	29.183	-81.048	12.5	-	52.20	38

Orlando Sanford Airport	FL	KSFB	28.78	-81.244	16.8	+	42.57	35
Jacksonville International A	FL	KJAX	30.495	-81.694	7.9	-	47.70	38
Jacksonville Nas	FL	KNIP	30.233	-81.667	6.1	-	39.96	37
Mayport Naf	FL	KNRB	30.4	-81.417	4.9	+	52.85	32
Cecil Field Airport	FL	KVQQ	30.219	-81.876	24.7	-	49.93	27
Jacksonville/Craig	FL	KCRG	30.336	-81.515	12.5	+	37.66	37
Savannah/Hilton Head Intl Air	GA	KSAV	32.13	-81.21	14	-	56.23	34
Charleston Afb/International	SC	KCHS	32.899	-80.04	12.2	+	56.57	38
Beaufort Mcas	SC	KNBC	32.483	-80.717	11.3	+	50.08	36
Wright Aaf Airport	GA	KLHW	31.883	-81.567	13.7	+	54.01	28
St Lucie County Intl Arpt	FL	KFPR	27.498	-80.377	7.3	+	39.49	23
Albert Whitted Airport	FL	KSPG	27.765	-82.628	2.4	+	45.14	25
Page Field Airport	FL	KFMY	26.585	-81.861	4.6	-	53.74	35
Sw Florida Intn Airport	FL	KRSW	26.536	-81.755	9.5	+	41.47	27
Tampa International Airport	FL	KTPA	27.962	-82.54	5.8	-	47.22	38
Sarasota/Bradenton Intl Ap	FL	KSRQ	27.401	-82.559	8.5	-	38.47	38
St Pete-Clwtr Intl Airport	FL	KPIE	27.911	-82.688	3.4	+	44.74	38
Alma/Bacon Co.	GA	KAMG	31.536	-82.507	62.8	-	38.18	37
Malcolm Mc Kinnon Airport	GA	KSSI	31.152	-81.391	4.9	+	36.10	38
Tallahassee Regional Airport	FL	KTLH	30.393	-84.353	16.8	-	39.46	38
Gainesville Rgnl	FL	KGNV	29.692	-82.276	50.3	+	37.46	38
Valdosta Regional Airport	GA	KVLD	30.783	-83.277	60.4	-	36.34	38
Eglin Afb Airport	FL	KVPS	30.483	-86.517	26.5	+	42.92	33
Bob Sikes Airport	FL	KCEW	30.78	-86.523	57.9	+	50.95	36
Pensacola Regional Airport	FL	KPNS	30.478	-87.187	34.1	-	41.34	38
Pensacola Nas	FL	KNPA	30.35	-87.317	8.5	-	47.90	20
Whiting Field Naval Air Stati	FL	KNSE	30.717	-87.017	60.7	-	43.27	34
Panama City-Bay Co. Int Ap	FL	KPFN	30.212	-85.683	6.4	+	44.34	28
Eglin Af Aux Nr 3 D	FL	KEGI	30.65	-86.517	58	+	38.44	30
Wilmington Intl	NC	KILM	34.268	-77.9	11.6	-	48.81	26
Pope Afb Airport	NC	KPOB	35.174	-79.009	66.5	+	55.51	20
Fayett Rgnl/Grannis Fld Ap	NC	KFAY	34.991	-78.88	56.7	+	49.41	39
Cape Hatteras	NC	KHSE	35.233	-75.622	3.4	-	48.51	37
Seymour-Johnson Afb Airport	NC	KGSB	35.344	-77.965	33.2	+	50.96	23
Rocky Mount-Wilson Rgn Apt	NC	KRWI	35.855	-77.893	48.8	+	43.71	38
Oceana Nas	VA	KNTU	36.817	-76.033	7	+	47.64	37
Norfolk International Airport	VA	KORF	36.903	-76.192	9.1	-	49.56	36
Norfolk Nas	VA	KNGU	36.937	-76.289	5.2	-	49.36	38
Cherry Point Mcas	NC	KNKT	34.9	-76.883	8.8	+	45.21	38
Craven County Reg Airport	NC	KEWN	35.068	-77.048	5.8	-	44.38	35
Jacksonville	NC	KNCA	34.708	-77.44	7.9	+	41.72	38
Columbia Metropolitan Airport	SC	KCAE	33.942	-81.118	68.6	+	51.34	35
Mcentire Air National Guard S	SC	KMMT	33.967	-80.8	77.4	+	47.41	38

Florence Regional Airport	SC	KFLO	34.185	-79.724	44.5	+	49.91	29
Wallops Flight Facility Airpo	VA	KWAL	37.937	-75.471	14	+	43.67	38
Salisbury Ocean Cit	MD	KSBY	38.341	-75.51	18.3	-	43.76	25
Atlantic City International A	NJ	KACY	39.449	-74.567	18.3	-	64.52	38
Millville Municipal Arpt	NJ	KMIV	39.367	-75.067	21.3	+	58.46	38
Naes/Maxfield Field	NJ	KNEL	40.033	-74.35	30.8	+	50.91	38
La Guardia Airport	NY	KLGA	40.779	-73.88	3.4	+	48.85	30
Long Island Mac Art	NY	KISP	40.794	-73.102	30.2	+	37.76	18
Westchester County Airport	NY	KHPN	41.067	-73.708	115.5	-	61.55	37
Igor I Sikorsky Memorial Airp	CT	KBDR	41.158	-73.129	1.5	+	55.30	38
Groton-New London Airport	CT	KGON	41.328	-72.049	3.1	+	39.64	38
New Bedford Rgnl Airport	MA	KEWB	41.676	-70.958	24.4	+	56.53	38
Marthas Vineyard Airport	MA	KMVY	41.393	-70.615	20.7	+	45.14	38
Brnsbl Muni-Bman/Pol Fd Ap	MA	KHYA	41.669	-70.28	16.8	+	64.38	21
Theodore F Green State Airpor	RI	KPVD	41.723	-71.433	16.8	-	45.60	20
Bradley International Airport	CT	KBDL	41.938	-72.682	53.3	+	43.88	38
Danbury Municipal Airport	CT	KDXR	41.371	-73.483	139.3	+	51.80	38
Hartford-Brainard Airport	CT	KHFD	41.736	-72.651	5.8	+	66.51	38
Beverly Municipal Airport	MA	KBVY	42.584	-70.918	32.9	+	51.06	38
Gen E L Logan International A	MA	KBOS	42.361	-71.01	3.7	+	44.68	38
Norwood Memorial Airport	MA	KOWD	42.191	-71.174	15.2	-	43.08	30
Concord Municipal Airport	NH	KCON	43.12	-71.3	105.5	+	47.05	36
Pease International Tradeport	NH	KPSM	43.083	-70.817	30.5	+	38.76	35
Portland International Jetpor	ME	KPWM	43.65	-70.3	13.7	+	62.78	38
Naval Air Station	ME	KNHZ	43.9	-69.933	21.3	-	75.40	21
Manchester Airport	NH	KMHT	42.933	-71.438	68.6	+	43.53	38
John F Kennedy International	NY	KJFK	40.639	-73.762	3.4	-	46.49	34
Lawrence Municipal Airport	MA	KLWM	42.717	-71.124	45.4	+	58.31	40
Westover Afb/Metropolitan Air	MA	KCEF	42.2	-72.533	73.5	+	50.60	38
Barnes Municipal Airport	MA	KBAF	42.158	-72.716	82.6	+	46.69	37
Langley Afb Airport	VA	KLFI	37.083	-76.36	3.1	-	57.30	38
Simmons Aaf Airport	NC	KFBG	35.133	-78.933	74.4	+	52.66	38
Elizabeth City Cgas	NC	KECG	36.261	-76.175	4	+	53.97	18
Tyndall Afb Airport	FL	KPAM	30.067	-85.583	5.2	-	61.91	31
Hurlburt Field Airport	FL	KHRT	30.417	-86.683	11.6	-	54.55	22
Hunter Army Airfield	GA	KSVN	32.017	-81.133	12.5	-	62.39	28
Mac Dill Afb Airport	FL	KMCF	27.85	-82.517	4.3	+	35.63	18
Shaw Air Force Base	SC	KSSC	33.967	-80.467	73.5	+	54.17	39
Grand Strand Airport	SC	KCRE	33.812	-78.724	9.8	-	49.96	37
Kennedy Space Center	FL	KTTS	28.617	-80.683	3.1	+	47.59	40
Patrick Afb Airport	FL	KCOF	28.233	-80.6	2.4	+	44.48	37

Table A.3. Sites used, thunderstorm data stations

Thunderstorms								
STATION NAME	ST	CODE	LAT	LON	ELEV (m)	SIGN	MEAN	N
Key West International Airpor	FL	KEYW	24.555	-81.752	1.2	-	51.44	38
Key West Nas	FL	KNQX	24.583	-81.683	1.8	+	54.70	32
Miami International Airport	FL	KMIA	25.791	-80.316	8.8	+	51.23	38
Opa Locka Airport	FL	KOPF	25.907	-80.28	3.1	+	36.34	24
Fort Lauderdale Hol	FL	KFLL	26.072	-80.154	3.4	-	45.23	35
Homestead Afb Airport	FL	KHST	25.483	-80.383	1.5	-	40.64	23
Kendall-Tamiami Exec Arpt	FL	KTMB	25.648	-80.433	3.1	+	37.22	26
Palm Beach International Airp	FL	KPBI	26.685	-80.099	5.8	-	53.14	34
Ft Lauder Executive Arpt	FL	KFXE	26.197	-80.171	4.3	-	48.82	26
Melbourne Intl Ap	FL	KMLB	28.101	-80.644	8.2	+	61.19	36
Vero Beach Muni	FL	KVRB	27.653	-80.243	8.5	+	69.04	38
Pompano Beach Airpark Arpt	FL	KPMP	26.25	-80.108	6.4	+	37.32	22
Orlando International Airport	FL	KMCO	28.434	-81.325	27.4	+	52.29	38
Executive Airport	FL	KORL	28.545	-81.333	32.9	+	73.79	21
Daytona Beach Intl	FL	KDAB	29.183	-81.048	12.5	-	52.66	38
Orlando Sanford Airport	FL	KSFB	28.78	-81.244	16.8	+	45.43	29
Jacksonville International A	FL	KJAX	30.495	-81.694	7.9	-	47.45	38
Jacksonville Nas	FL	KNIP	30.233	-81.667	6.1	-	50.84	37
Mayport Naf	FL	KNRB	30.4	-81.417	4.9	+	40.98	24
Cecil Field Airport	FL	KVQQ	30.219	-81.876	24.7	-	41.43	25
Jacksonville/Craig	FL	KCRG	30.336	-81.515	12.5	+	47.26	35
Savannah/Hilton Head Intl Air	GA	KSAV	32.13	-81.21	14	-	53.52	34
Charleston Afb/International	SC	KCHS	32.899	-80.04	12.2	+	49.57	38
Beaufort Mcas	SC	KNBC	32.483	-80.717	11.3	+	34.80	36
Wright Aaf Airport	GA	KLHW	31.883	-81.567	13.7	+	55.06	26
St Lucie County Intl Arpt	FL	KFPR	27.498	-80.377	7.3	+	41.16	23
Albert Whitted Airport	FL	KSPG	27.765	-82.628	2.4	+	39.61	25
Page Field Airport	FL	KFMY	26.585	-81.861	4.6	-	50.79	34
Sw Florida Intn Airport	FL	KRSW	26.536	-81.755	9.5	+	39.98	27
Tampa International Airport	FL	KTPA	27.962	-82.54	5.8	-	42.56	38
Sarasota/Bradenton Intl Ap	FL	KSRQ	27.401	-82.559	8.5	-	52.94	38
St Pete-Clwtr Intl Airport	FL	KPIE	27.911	-82.688	3.4	+	56.89	38
Alma/Bacon Co.	GA	KAMG	31.536	-82.507	62.8	-	35.97	35
Malcolm Mc Kinnon Airport	GA	KSSI	31.152	-81.391	4.9	+	36.71	37
Tallahassee Regional Airport	FL	KTLH	30.393	-84.353	16.8	-	54.25	38
Gainesville Rgnl	FL	KGNV	29.692	-82.276	50.3	+	35.69	38
Valdosta Regional Airport	GA	KVLD	30.783	-83.277	60.4	-	39.96	38

Eglin Afb Airport	FL	KVPS	30.483	-86.517	26.5	+	48.86	36
Bob Sikes Airport	FL	KCEW	30.78	-86.523	57.9	+	43.76	37
Pensacola Regional Airport	FL	KPNS	30.478	-87.187	34.1	-	39.08	20
Pensacola Nas	FL	KNPA	30.35	-87.317	8.5	-	40.19	34
Whiting Field Naval Air Stati	FL	KNSE	30.717	-87.017	60.7	-	44.04	28
Panama City-Bay Co. Int Ap	FL	KPFN	30.212	-85.683	6.4	+	43.22	28
Eglin Af Aux Nr 3 D	FL	KEGI	30.65	-86.517	58	+	38.38	25
Wilmington Intl	NC	KILM	34.268	-77.9	11.6	-	44.48	20
Pope Afb Airport	NC	KPOB	35.174	-79.009	66.5	+	47.35	34
Fayett Rgnl/Grannis Fld Ap	NC	KFAY	34.991	-78.88	56.7	+	53.09	36
Cape Hatteras	NC	KHSE	35.233	-75.622	3.4	-	48.19	23
Seymour-Johnson Afb Airport	NC	KGSB	35.344	-77.965	33.2	+	40.38	36
Rocky Mount-Wilson Rgn Apt	NC	KRWI	35.855	-77.893	48.8	+	51.57	33
Oceana Nas	VA	KNTU	36.817	-76.033	7	+	37.17	33
Norfolk International Airport	VA	KORF	36.903	-76.192	9.1	-	64.24	38
Norfolk Nas	VA	KNGU	36.937	-76.289	5.2	-	41.66	38
Cherry Point Mcas	NC	KNKT	34.9	-76.883	8.8	+	47.42	35
Craven County Reg Airport	NC	KEWN	35.068	-77.048	5.8	-	39.92	37
Jacksonville	NC	KNCA	34.708	-77.44	7.9	+	36.45	32
Columbia Metropolitan Airport	SC	KCAE	33.942	-81.118	68.6	+	46.74	38
Mcentire Air National Guard S	SC	KMMT	33.967	-80.8	77.4	+	48.82	25
Florence Regional Airport	SC	KFLO	34.185	-79.724	44.5	+	46.49	36
Wallops Flight Facility Airpo	VA	KWAL	37.937	-75.471	14	+	40.77	18
Salisbury Ocean Cit	MD	KSBY	38.341	-75.51	18.3	-	43.10	32
Atlantic City International A	NJ	KACY	39.449	-74.567	18.3	-	48.43	33
Millville Municipal Arpt	NJ	KMIV	39.367	-75.067	21.3	+	45.21	34
Naes/Maxfield Field	NJ	KNEL	40.033	-74.35	30.8	+	58.93	21
La Guardia Airport	NY	KLGA	40.779	-73.88	3.4	+	42.24	37
Long Island Mac Art	NY	KISP	40.794	-73.102	30.2	+	55.42	37
Westchester County Airport	NY	KHPN	41.067	-73.708	115.5	-	44.43	36
Igor I Sikorsky Memorial Airp	CT	KBDR	41.158	-73.129	1.5	+	55.81	31
Groton-New London Airport	CT	KGON	41.328	-72.049	3.1	+	45.42	33
New Bedford Rgnl Airport	MA	KEWB	41.676	-70.958	24.4	+	32.11	29
Marthas Vineyard Airport	MA	KMVY	41.393	-70.615	20.7	+	42.76	24
Brnsbl Muni-Bman/Pol Fd Ap	MA	KHYA	41.669	-70.28	16.8	+	42.53	29
Theodore F Green State Airpor	RI	KPVD	41.723	-71.433	16.8	-	41.20	38
Bradley International Airport	CT	KBDL	41.938	-72.682	53.3	+	52.24	38
Danbury Municipal Airport	CT	KDXR	41.371	-73.483	139.3	+	31.95	24
Hartford-Brainard Airport	CT	KHFD	41.736	-72.651	5.8	+	39.80	33
Beverly Municipal Airport	MA	KBVY	42.584	-70.918	32.9	+	30.89	32
Gen E L Logan International A	MA	KBOS	42.361	-71.01	3.7	+	43.86	38
Norwood Memorial Airport	MA	KOWD	42.191	-71.174	15.2	-	40.58	28
Concord Municipal Airport	NH	KCON	43.12	-71.3	105.5	+	39.76	31

Pease International Tradeport	NH	KPSM	43.083	-70.817	30.5	+	52.92	26
Portland International Jetpor	ME	KPWM	43.65	-70.3	13.7	+	49.08	32
Naval Air Station	ME	KNHZ	43.9	-69.933	21.3	-	44.11	23
Manchester Airport	NH	KMHT	42.933	-71.438	68.6	+	40.00	29
John F Kennedy International	NY	KJFK	40.639	-73.762	3.4	-	40.21	38
Lawrence Municipal Airport	MA	KLWM	42.717	-71.124	45.4	+	47.09	26
Westover Afb/Metropolitan Air	MA	KCEF	42.2	-72.533	73.5	+	48.03	26
Barnes Municipal Airport	MA	KBAF	42.158	-72.716	82.6	+	56.21	28
Langley Afb Airport	VA	KLFI	37.083	-76.36	3.1	-	49.91	39
Simmons Aaf Airport	NC	KFBG	35.133	-78.933	74.4	+	54.67	35
Elizabeth City Cgas	NC	KECG	36.261	-76.175	4	+	69.10	19
Tyndall Afb Airport	FL	KPAM	30.067	-85.583	5.2	-	46.36	32
Hurlburt Field Airport	FL	KHRT	30.417	-86.683	11.6	-	44.15	32
Hunter Army Airfield	GA	KSVN	32.017	-81.133	12.5	-	41.06	31
Mac Dill Afb Airport	FL	KMCF	27.85	-82.517	4.3	+	57.18	30
Shaw Air Force Base	SC	KSSC	33.967	-80.467	73.5	+	50.81	36
Grand Strand Airport	SC	KCRE	33.812	-78.724	9.8	-	46.59	32
Kennedy Space Center	FL	KTTS	28.617	-80.683	3.1	+	54.48	18
Patrick Afb Airport	FL	KCOF	28.233	-80.6	2.4	+	44.24	36

Table A.4. Sites used, tropical storm data stations

Tropical Storms

STATION NAME	ST	CODE	LAT	LON	ELEV (m)	SIGN	MEAN	N
Key West International Airpor	FL	KEYW	24.555	-81.752	1.2	+	40.85	14
Hernando County Airport	FL	KBKV	28.474	-82.454	1.8	+	57.61	8
Key West Nas	FL	KNQX	24.583	-81.683	8.8	-	45.07	11
The Fl Keys Marathon Arpt	FL	KMTH	24.726	-81.052	3.1	+	74.06	6
Miami International Airport	FL	KMIA	25.791	-80.316	3.4	+	48.76	18
Opa Locka Airport	FL	KOPF	25.907	-80.28	1.5	-	47.55	8
Fort Lauderdale Hol	FL	KFLL	26.072	-80.154	3.1	+	43.40	14
Homestead Afb Airport	FL	KHST	25.483	-80.383	5.8	-	37.10	11
Kendall-Tamiami Exec Arpt	FL	KTMB	25.648	-80.433	4.3	+	68.35	10
Palm Beach International Airp	FL	KPBI	26.685	-80.099	8.2	+	38.77	16
Charlotte County Airport	FL	KPGD	26.917	-81.991	8.5	-	29.37	8
North Perry Airport	FL	KHWO	25.999	-80.241	6.4	-	43.81	5
Naples Municipal Airport	FL	KAPF	26.152	-81.775	27.4	-	46.36	8
Ft Lauder Executive Arpt	FL	KFXE	26.197	-80.171	32.9	+	38.96	10
Melbourne Intl Ap	FL	KMLB	28.101	-80.644	12.5	+	79.06	15
Vero Beach Muni	FL	KVRB	27.653	-80.243	16.8	+	59.87	17
Pompano Beach Airpark Arpt	FL	KPMP	26.25	-80.108	7.9	+	35.97	9

Orlando International Airport	FL	KMCO	28.434	-81.325	6.1	+	52.69	16
Executive Airport	FL	KORL	28.545	-81.333	4.9	+	66.85	11
Daytona Beach Intl	FL	KDAB	29.183	-81.048	24.7	+	49.56	20
Orlando Sanford Airport	FL	KSFB	28.78	-81.244	12.5	+	60.68	13
Jacksonville International A	FL	KJAX	30.495	-81.694	14	+	53.67	16
Jacksonville Nas	FL	KNIP	30.233	-81.667	12.2	+	47.85	14
Mayport Naf	FL	KNRB	30.4	-81.417	11.3	-	60.13	14
Cecil Field Airport	FL	KVQQ	30.219	-81.876	13.7	+	36.66	5
Jacksonville/Craig	FL	KCRG	30.336	-81.515	7.3	+	49.10	12
Destin-Ft.Walton Beach Apt	FL	KDTS	30.4	-86.472	2.4	+	50.42	8
Savannah/Hilton Head Intl Air	GA	KSAV	32.13	-81.21	4.6	-	34.24	12
Charleston Afb/International	SC	KCHS	32.899	-80.04	9.5	+	68.16	19
Beaufort Mcas	SC	KNBC	32.483	-80.717	5.8	-	39.33	10
Wright Aaf Airport	GA	KLHW	31.883	-81.567	8.5	+	40.05	5
St Lucie County Intl Arpt	FL	KFPR	27.498	-80.377	3.4	+	38.89	11
Albert Whitted Airport	FL	KSPG	27.765	-82.628	62.8	-	50.25	13
Page Field Airport	FL	KFMY	26.585	-81.861	4.9	+	37.07	13
Sw Florida Intn Airport	FL	KRSW	26.536	-81.755	16.8	+	35.62	12
Tampa International Airport	FL	KTPA	27.962	-82.54	50.3	-	37.35	15
Sarasota/Bradenton Intl Ap	FL	KSRQ	27.401	-82.559	60.4	-	41.04	18
St Pete-Clwtr Intl Airport	FL	KPIE	27.911	-82.688	26.5	-	43.83	16
Cross City Airport	FL	KCTY	29.633	-83.105	57.9	+	39.32	8
Alma/Bacon Co.	GA	KAMG	31.536	-82.507	34.1	+	42.95	8
Malcolm Mc Kinnon Airport	GA	KSSI	31.152	-81.391	8.5	+	37.54	14
Tallahassee Regional Airport	FL	KTLH	30.393	-84.353	60.7	-	42.63	13
Gainesville Rgnl	FL	KGNV	29.692	-82.276	6.4	+	44.93	13
Valdosta Regional Airport	GA	KVLD	30.783	-83.277	58	+	59.06	9
Apalachicola Muni Airport	FL	KAAF	29.733	-85.033	11.6	-	67.15	8
Eglin Afb Airport	FL	KVPS	30.483	-86.517	66.5	+	73.10	14
Leesburg Regional Airport	FL	KLEE	28.821	-81.81	56.7	+	56.52	7
Bob Sikes Airport	FL	KCEW	30.78	-86.523	3.4	-	64.02	14
Pensacola Regional Airport	FL	KPNS	30.478	-87.187	33.2	-	48.63	9
Perry Foley	FL	K40J	30.072	-83.574	48.8	+	65.18	7
Pensacola Nas	FL	KNPA	30.35	-87.317	7	-	31.64	11
Whiting Field Naval Air Stati	FL	KNSE	30.717	-87.017	9.1	-	52.34	9
Panama City-Bay Co. Int Ap	FL	KPFN	30.212	-85.683	5.2	-	46.12	11
Eglin Af Aux Nr 3 D	FL	KEGI	30.65	-86.517	8.8	-	63.61	5
Wilmington Intl	NC	KILM	34.268	-77.9	5.8	+	85.99	13
Pope Afb Airport	NC	KPOB	35.174	-79.009	7.9	+	41.63	13
Fayett Rgnl/Grannis Fld Ap	NC	KFAY	34.991	-78.88	68.6	+	49.80	13
Michael J Smith Fld Arpt	NC	KMRH	34.734	-76.661	77.4	+	73.36	7
Cape Hatteras	NC	KHSE	35.233	-75.622	44.5	+	50.78	13
Seymour-Johnson Afb Airport	NC	KGSB	35.344	-77.965	14	+	99.29	10

Rocky Mount-Wilson Rgn Apt	NC	KRWI	35.855	-77.893	18.3	+	65.86	10
Oceana Nas	VA	KNTU	36.817	-76.033	18.3	+	52.25	20
Norfolk International Airport	VA	KORF	36.903	-76.192	21.3	+	50.70	22
Norfolk Nas	VA	KNGU	36.937	-76.289	30.8	+	53.76	18
Cherry Point Mcas	NC	KNKT	34.9	-76.883	3.4	+	56.76	21
Craven County Reg Airport	NC	KEWN	35.068	-77.048	30.2	+	43.84	12
Jacksonville	NC	KNCA	34.708	-77.44	115.5	+	50.25	16
Columbia Metropolitan Airport	SC	KCAE	33.942	-81.118	1.5	-	35.43	11
Florence Regional Airport	SC	KFLO	34.185	-79.724	3.1	-	37.10	11
Lumberton Municipal Arpt	NC	KLBT	34.608	-79.059	24.4	-	44.57	5
Laurinburg-Maxton Airport	NC	KMEB	34.792	-79.366	20.7	-	36.35	5
Billy Mitchell Airport	NC	KHSE	35.233	-75.622	16.8	-	61.40	14
Wallops Flight Facility Airpo	VA	KWAL	37.937	-75.471	16.8	+	72.39	10
Salisbury Ocean Cit	MD	KSBY	38.341	-75.51	53.3	+	75.57	14
Atlantic City International A	NJ	KACY	39.449	-74.567	139.3	-	29.52	14
Millville Municipal Arpt	NJ	KMIV	39.367	-75.067	5.8	-	55.79	10
Sussex County Airport	DE	KGED	38.689	-75.359	32.9	+	53.48	6
La Guardia Airport	NY	KLGA	40.779	-73.88	3.7	-	50.04	11
Long Island Mac Art	NY	KISP	40.794	-73.102	15.2	-	34.12	10
Westchester County Airport	NY	KHPN	41.067	-73.708	105.5	-	38.60	7
Igor I Sikorsky Memorial Airp	CT	KBDR	41.158	-73.129	30.5	-	30.64	10
Groton-New London Airport	CT	KGON	41.328	-72.049	13.7	-	30.63	7
Nantucket Mem	MA	KACK	41.253	-70.061	21.3	-	51.78	12
Plymouth Municipal Airport	MA	KPYM	41.91	-70.729	68.6	+	38.04	7
New Bedford Rgnl Airport	MA	KEWB	41.676	-70.958	3.4	+	72.45	6
Marthas Vineyard Airport	MA	KMVY	41.393	-70.615	45.4	+	49.05	14
Brnsbl Muni-Bman/Pol Fd Ap	MA	KHYA	41.669	-70.28	73.5	+	61.06	12
Chatham Municipal Airport	MA	KCQX	41.688	-69.993	82.6	+	62.46	5
Theodore F Green State Airpor	RI	KPVD	41.723	-71.433	3.1	-	38.90	9
Bradley International Airport	CT	KBDL	41.938	-72.682	74.4	-	40.46	8
Hartford-Brainard Airport	CT	KHFD	41.736	-72.651	4	+	82.46	5
Beverly Municipal Airport	MA	KBVY	42.584	-70.918	5.2	+	74.08	5
Gen E L Logan International A	MA	KBOS	42.361	-71.01	11.6	-	50.68	8
Concord Municipal Airport	NH	KCON	43.12	-71.3	12.5	+	60.88	6
Pease International Tradeport	NH	KPSM	43.083	-70.817	4.3	+	82.78	8
Portland International Jetpor	ME	KPWM	43.65	-70.3	73.5	-	23.41	7
Manchester Airport	NH	KMHT	42.933	-71.438	9.8	-	42.82	6
John F Kennedy International	NY	KJFK	40.639	-73.762	3.1	-	32.22	9
Francis S Gabreski Ap	NY	KFOK	40.844	-72.632	2.4	-	42.94	8
Bedford Hanscom Field	MA	KBED	42.47	-71.289	40.5	-	46.55	5
Westover Afb/Metropolitan Air	MA	KCEF	42.2	-72.533	73.5	+	87.84	7
Barnes Municipal Airport	MA	KBAF	42.158	-72.716	82.6	+	73.20	5
Ocean City Municipal Artp	MD	KOXB	38.308	-75.124	3.7	+	41.57	6

Langley Afb Airport	VA	KLFI	37.083	-76.36	3.1	+	50.69	17
Simmons Aaf Airport	NC	KFBG	35.133	-78.933	74.4	+	54.49	14
Elizabeth City Cgas	NC	KECG	36.261	-76.175	4	+	41.41	15
Tyndall Afb Airport	FL	KPAM	30.067	-85.583	5.2	-	50.22	13
Marianna Municipal Airport	FL	KMAI	30.836	-85.184	34.4	-	37.65	5
Hurlburt Field Airport	FL	KHRT	30.417	-86.683	11.6	+	78.19	11
Hunter Army Airfield	GA	KSVN	32.017	-81.133	12.5	-	46.72	14
Mac Dill Afb Airport	FL	KMCF	27.85	-82.517	4.3	+	71.80	13
Shaw Air Force Base	SC	KSSC	33.967	-80.467	73.5	-	47.04	9
Myrtle Beach Intl Airport	SC	KMYR	33.683	-78.933	7.6	+	51.27	5
Grand Strand Airport	SC	KCRE	33.812	-78.724	9.8	+	43.62	16
Nasa Shuttle Fclty	FL	KSC	28.617	-80.7	3	-	44.87	6
Kennedy Space Center	FL	KTTS	28.617	-80.683	3.1	+	55.57	11
Patrick Afb Airport	FL	KCOF	28.233	-80.6	2.4	+	46.78	17

Table A.5. Significance Statistics for Commingled Stations

Commingled								
Station Name	ST	CODE	LAT	LON	SIGN	N	MK	T
Key West International Airpor	FL	KEYW	24.555	-81.752	P	38	0.860	0.223
Key West Nas	FL	KNQX	24.583	-81.683	P	34	0.678	0.303
Miami International Airport	FL	KMIA	25.791	-80.316	P	38	0.183	0.074
Opa Locka Airport	FL	KOPF	25.907	-80.28	P	24	0.000	0.000
Fort Lauderdale Hol	FL	KFLL	26.072	-80.154	P	38	0.633	0.235
Homestead Afb Airport	FL	KHST	25.483	-80.383	N	27	0.934	0.687
Kendall-Tamiami Exec Arpt	FL	KTMB	25.648	-80.433	P	27	0.050	0.043
Palm Beach International Airp	FL	KPBI	26.685	-80.099	P	35	0.609	0.393
Ft Lauder Executive Arpt	FL	KFXE	26.197	-80.171	P	27	0.588	0.286
Melbourne Intl Ap	FL	KMLB	28.101	-80.644	P	37	0.038	0.048
Vero Beach Muni	FL	KVRB	27.653	-80.243	N	38	0.669	0.571
Pompano Beach Airpark Arpt	FL	KPMP	26.25	-80.108	P	22	0.159	0.035
Orlando International Airport	FL	KMCO	28.434	-81.325	P	38	0.339	0.108
Executive Airport	FL	KORL	28.545	-81.333	P	21	0.110	0.146
Daytona Beach Intl	FL	KDAB	29.183	-81.048	N	38	0.436	0.696
Orlando Sanford Airport	FL	KSFB	28.78	-81.244	P	35	0.000	0.000
Jacksonville International A	FL	KJAX	30.495	-81.694	N	38	0.209	0.881
Jacksonville Nas	FL	KNIP	30.233	-81.667	P	37	0.647	0.432
Mayport Naf	FL	KNRB	30.4	-81.417	P	32	0.733	0.314
Cecil Field Airport	FL	KVQQ	30.219	-81.876	N	27	0.646	0.732

Jacksonville/Craig	FL	KCRG	30.336	-81.515	P	37	0.001	0.001
Savannah/Hilton Head Intl Air	GA	KSAV	32.13	-81.21	N	34	0.085	0.966
Charleston Afb/International	SC	KCHS	32.899	-80.04	P	38	0.597	0.314
Beaufort Mcas	SC	KNBC	32.483	-80.717	P	36	0.577	0.354
Wright Aaf Airport	GA	KLHW	31.883	-81.567	N	28	0.890	0.546
St Lucie County Intl Arpt	FL	KFPR	27.498	-80.377	P	23	0.170	0.184
Albert Whitted Airport	FL	KSPG	27.765	-82.628	P	25	0.154	0.097
Page Field Airport	FL	KFMY	26.585	-81.861	P	35	0.293	0.051
Sw Florida Intn Airport	FL	KRSW	26.536	-81.755	P	27	0.095	0.022
Tampa International Airport	FL	KTPA	27.962	-82.54	N	38	0.113	0.953
Sarasota/Bradenton Intl Ap	FL	KSRQ	27.401	-82.559	P	38	0.113	0.071
St Pete-Clwtr Intl Airport	FL	KPIE	27.911	-82.688	P	38	0.108	0.026
Alma/Bacon Co.	GA	KAMG	31.536	-82.507	N	37	0.647	0.755
Malcolm Mc Kinnon Airport	GA	KSSI	31.152	-81.391	P	38	0.087	0.028
Tallahassee Regional Airport	FL	KTLH	30.393	-84.353	P	38	0.669	0.424
Gainesville Rgnl	FL	KGNV	29.692	-82.276	P	38	0.597	0.307
Valdosta Regional Airport	GA	KVLD	30.783	-83.277	N	38	0.303	0.956
Apalachicola Muni Airport	FL	KAAF	29.733	-85.033	P	33	0.001	0.006
Eglin Afb Airport	FL	KVPS	30.483	-86.517	P	36	0.376	0.143
Bob Sikes Airport	FL	KCEW	30.78	-86.523	P	38	0.011	0.010
Pensacola Regional Airport	FL	KPNS	30.478	-87.187	P	20	0.820	0.496
Pensacola Nas	FL	KNPA	30.35	-87.317	P	34	0.635	0.373
Whiting Field Naval Air Stati	FL	KNSE	30.717	-87.017	N	28	0.678	0.608
Panama City-Bay Co. Int Ap	FL	KPFN	30.212	-85.683	P	30	0.015	0.014
Eglin Af Aux Nr 3 D	FL	KEGI	30.65	-86.517	P	26	0.290	0.212
Wilmington Intl	NC	KILM	34.268	-77.9	P	20	0.770	0.489
Pope Afb Airport	NC	KPOB	35.174	-79.009	P	39	0.276	0.205
Fayett Rgnl/Grannis Fld Ap	NC	KFAY	34.991	-78.88	P	37	0.077	0.043
Cape Hatteras	NC	KHSE	35.233	-75.622	P	23	0.342	0.113
Seymour-Johnson Afb Airport	NC	KGSB	35.344	-77.965	P	38	0.481	0.124
Rocky Mount-Wilson Rgn Apt	NC	KRWI	35.855	-77.893	P	37	0.048	0.024
Oceana Nas	VA	KNTU	36.817	-76.033	P	36	0.007	0.005
Norfolk International Airport	VA	KORF	36.903	-76.192	N	38	0.200	0.850
Norfolk Nas	VA	KNGU	36.937	-76.289	P	38	0.258	0.228
Cherry Point Mcas	NC	KNKT	34.9	-76.883	P	35	0.001	0.003
Craven County Reg Airport	NC	KEWN	35.068	-77.048	N	38	0.687	0.685
Jacksonville	NC	KNCA	34.708	-77.44	P	35	0.053	0.026
Columbia Metropolitan Airport	SC	KCAE	33.942	-81.118	N	38	0.706	0.553
Mcentire Air National Guard S	SC	KMMT	33.967	-80.8	P	29	0.026	0.009
Florence Regional Airport	SC	KFLO	34.185	-79.724	P	38	0.108	0.040
Wallops Flight Facility Airpo	VA	KWAL	37.937	-75.471	P	25	0.005	0.007
Salisbury Ocean Cit	MD	KSBY	38.341	-75.51	N	38	0.615	0.534
Atlantic City International A	NJ	KACY	39.449	-74.567	N	38	0.980	0.661

Millville Municipal Arpt	NJ	KMIV	39.367	-75.067	N	38	0.669	0.824
Naes/Maxfield Field	NJ	KNEL	40.033	-74.35	P	30	0.544	0.319
Sussex County Airport	DE	KGED	38.689	-75.359	P	18	0.034	0.017
La Guardia Airport	NY	KLGA	40.779	-73.88	N	37	0.327	0.814
Long Island Mac Art	NY	KISP	40.794	-73.102	N	38	0.191	0.926
Westchester County Airport	NY	KHPN	41.067	-73.708	P	38	0.379	0.329
Igor I Sikorsky Memorial Airp	CT	KBDR	41.158	-73.129	N	38	0.218	0.761
Groton-New London Airport	CT	KGON	41.328	-72.049	N	38	0.247	0.929
Nantucket Mem	MA	KACK	41.253	-70.061	N	21	0.097	0.756
Plymouth Municipal Airport	MA	KPYM	41.91	-70.729	P	20	0.581	0.297
New Bedford Rgnl Airport	MA	KEWB	41.676	-70.958	P	38	0.005	0.007
Marthas Vineyard Airport	MA	KMVY	41.393	-70.615	P	38	0.010	0.001
Brnsbl Muni-Bman/Pol Fd Ap	MA	KHYA	41.669	-70.28	P	38	0.669	0.166
Theodore F Green State Airpor	RI	KPVD	41.723	-71.433	N	38	0.039	0.986
Bradley International Airport	CT	KBDL	41.938	-72.682	N	38	0.669	0.727
Danbury Municipal Airport	CT	KDXR	41.371	-73.483	P	30	0.002	0.134
Hartford-Brainard Airport	CT	KHFD	41.736	-72.651	N	36	0.178	0.900
Beverly Municipal Airport	MA	KBVY	42.584	-70.918	P	35	0.027	0.034
Gen E L Logan International A	MA	KBOS	42.361	-71.01	N	38	0.003	0.990
Naval Air Station	MA	KNZW	42.15	-70.933	N	21	0.740	0.750
Norwood Memorial Airport	MA	KOWD	42.191	-71.174	P	38	0.763	0.495
Concord Municipal Airport	NH	KCON	43.12	-71.3	P	34	0.313	0.085
Pease International Tradeport	NH	KPSM	43.083	-70.817	N	40	0.012	0.979
Portland International Jetpor	ME	KPWM	43.65	-70.3	N	38	0.209	0.883
Naval Air Station	ME	KNHZ	43.9	-69.933	N	37	0.043	0.985
Manchester Airport	NH	KMHT	42.933	-71.438	P	38	0.421	0.210
John F Kennedy International	NY	KJFK	40.639	-73.762	N	38	0.113	0.895
Republic Airport	NY	KFRG	40.734	-73.417	N	18	0.112	0.982
Francis S Gabreski Ap	NY	KFOK	40.844	-72.632	N	31	0.001	0.999
Bedford Hanscom Field	MA	KBED	42.47	-71.289	N	22	0.003	0.999
Lawrence Municipal Airport	MA	KLWM	42.717	-71.124	P	28	0.594	0.486
Fort Devens/Ayer	MA	KAYE	42.567	-71.6	N	18	0.173	0.905
Westover Afb/Metropolitan Air	MA	KCEF	42.2	-72.533	N	39	0.127	0.920
Barnes Municipal Airport	MA	KBAF	42.158	-72.716	P	37	0.061	0.203
Langley Afb Airport	VA	KLFI	37.083	-76.36	N	40	0.268	0.815
Simmons Aaf Airport	NC	KFBG	35.133	-78.933	P	37	0.327	0.265

Table A.6. Significance Statistics for Nonthunderstorms Stations

Non-Thunderstorms								
Station_Na	ST	ID	LAT	LON	SIGN	N	MK	T
Key West International Airpor	FL	KEYW	24.555	-81.752	P	38	0.940	0.528
Key West Nas	FL	KNQX	24.583	-81.683	P	34	0.635	0.485
Miami International Airport	FL	KMIA	25.791	-80.316	N	38	0.407	0.481
Opa Locka Airport	FL	KOPF	25.907	-80.28	P	23	0.000	0.231
Fort Lauderdale Hol	FL	KFLL	26.072	-80.154	P	38	0.024	0.492
Homestead Afb Airport	FL	KHST	25.483	-80.383	N	27	0.227	0.160
Kendall-Tamiami Exec Arpt	FL	KTMB	25.648	-80.433	P	26	0.005	0.347
Palm Beach International Airp	FL	KPBI	26.685	-80.099	N	35	0.156	0.450
Ft Lauder Executive Arpt	FL	KFXE	26.197	-80.171	P	27	0.260	0.439
Melbourne Intl Ap	FL	KMLB	28.101	-80.644	P	37	0.301	0.345
Vero Beach Muni	FL	KVRB	27.653	-80.243	P	38	0.481	0.338
Pompano Beach Airpark Arpt	FL	KPMP	26.25	-80.108	P	21	0.085	0.471
Orlando International Airport	FL	KMCO	28.434	-81.325	P	38	0.393	0.462
Executive Airport	FL	KORL	28.545	-81.333	P	21	0.110	0.446
Daytona Beach Intl	FL	KDAB	29.183	-81.048	N	38	0.237	0.125
Orlando Sanford Airport	FL	KSFB	28.78	-81.244	P	34	0.000	0.409
Jacksonville International A	FL	KJAX	30.495	-81.694	N	38	0.339	0.009
Jacksonville Nas	FL	KNIP	30.233	-81.667	P	37	0.948	0.457
Mayport Naf	FL	KNRB	30.4	-81.417	P	32	0.189	0.487
Cecil Field Airport	FL	KVQQ	30.219	-81.876	P	27	0.835	0.132
Jacksonville/Craig	FL	KCRG	30.336	-81.515	P	36	0.015	0.304
Savannah/Hilton Head Intl Air	GA	KSAV	32.13	-81.21	N	34	0.091	0.000
Charleston Afb/International	SC	KCHS	32.899	-80.04	N	38	0.725	0.441
Beaufort Mcas	SC	KNBC	32.483	-80.717	P	36	0.294	0.445
Wright Aaf Airport	GA	KLHW	31.883	-81.567	N	28	0.567	0.412
St Lucie County Intl Arpt	FL	KFPR	27.498	-80.377	P	23	0.004	0.375
Albert Whitted Airport	FL	KSPG	27.765	-82.628	P	21	0.003	0.414
Page Field Airport	FL	KFMY	26.585	-81.861	P	35	0.050	0.478
Sw Florida Intn Airport	FL	KRSW	26.536	-81.755	P	25	0.042	0.421
Tampa International Airport	FL	KTPA	27.962	-82.54	P	38	0.044	0.001
Sarasota/Bradenton Intl Ap	FL	KSRQ	27.401	-82.559	P	37	0.205	0.424
St Pete-Clwtr Intl Airport	FL	KPIE	27.911	-82.688	P	38	0.008	0.476
Alma/Bacon Co.	GA	KAMG	31.536	-82.507	P	36	0.754	0.113
Malcolm Mc Kinnon Airport	GA	KSSI	31.152	-81.391	P	38	0.001	0.486
Tallahassee Regional Airport	FL	KTLH	30.393	-84.353	P	38	0.379	0.460
Gainesville Rgnl	FL	KGNV	29.692	-82.276	N	38	0.280	0.480
Valdosta Regional Airport	GA	KVLD	30.783	-83.277	N	37	0.224	0.001

Apalachicola Muni Airport	FL	KAAF	29.733	-85.033	P	33	0.000	0.292
Eglin Afb Airport	FL	KVPS	30.483	-86.517	P	35	0.776	0.483
Bob Sikes Airport	FL	KCEW	30.78	-86.523	P	38	0.047	0.383
Pensacola Regional Airport	FL	KPNS	30.478	-87.187	P	20	0.496	0.493
Pensacola Nas	FL	KNPA	30.35	-87.317	P	34	0.594	0.474
Whiting Field Naval Air Stati	FL	KNSE	30.717	-87.017	N	27	0.169	0.274
Panama City-Bay Co. Int Ap	FL	KPFN	30.212	-85.683	P	29	0.008	0.427
Eglin Af Aux Nr 3 D	FL	KEGI	30.65	-86.517	N	26	1.000	0.455
Wilmington Intl	NC	KILM	34.268	-77.9	P	20	0.183	0.390
Pope Afb Airport	NC	KPOB	35.174	-79.009	N	39	0.236	0.513
Fayett Rgnl/Grannis Fld Ap	NC	KFAY	34.991	-78.88	P	37	0.000	0.425
Cape Hatteras	NC	KHSE	35.233	-75.622	P	23	0.460	0.471
Seymour-Johnson Afb Airport	NC	KGSB	35.344	-77.965	P	38	0.841	0.496
Rocky Mount-Wilson Rgn Apt	NC	KRWI	35.855	-77.893	P	37	0.133	0.445
Oceana Nas	VA	KNTU	36.817	-76.033	P	36	0.000	0.452
Norfolk International Airport	VA	KORF	36.903	-76.192	N	38	0.119	0.021
Norfolk Nas	VA	KNGU	36.937	-76.289	P	38	0.379	0.456
Cherry Point Mcas	NC	KNKT	34.9	-76.883	P	35	0.001	0.418
Craven County Reg Airport	NC	KEWN	35.068	-77.048	N	38	0.530	0.188
Jacksonville	NC	KNCA	34.708	-77.44	P	35	0.021	0.355
Columbia Metropolitan Airport	SC	KCAE	33.942	-81.118	N	38	0.063	0.396
Mcentire Air National Guard S	SC	KMMT	33.967	-80.8	P	29	0.002	0.412
Florence Regional Airport	SC	KFLO	34.185	-79.724	P	38	0.119	0.458
Wallops Flight Facility Airpo	VA	KWAL	37.937	-75.471	P	25	0.008	0.496
Salisbury Ocean Cit	MD	KSBY	38.341	-75.51	N	38	0.481	0.415
Atlantic City International A	NJ	KACY	39.449	-74.567	P	38	0.597	0.210
Millville Municipal Arpt	NJ	KMIV	39.367	-75.067	N	38	0.421	0.046
Naes/Maxfield Field	NJ	KNEL	40.033	-74.35	P	30	0.887	0.504
Sussex County Airport	DE	KGED	38.689	-75.359	P	18	0.028	0.438
La Guardia Airport	NY	KLGA	40.779	-73.88	N	37	0.120	0.035
Long Island Mac Art	NY	KISP	40.794	-73.102	N	38	0.315	0.003
Westchester County Airport	NY	KHPN	41.067	-73.708	P	38	0.421	0.443
Igor I Sikorsky Memorial Airp	CT	KBDR	41.158	-73.129	N	38	0.145	0.061
Groton-New London Airport	CT	KGON	41.328	-72.049	N	38	0.218	0.002
Nantucket Mem	MA	KACK	41.253	-70.061	P	21	0.216	0.088
Plymouth Municipal Airport	MA	KPYM	41.91	-70.729	P	20	0.770	0.350
New Bedford Rgnl Airport	MA	KEWB	41.676	-70.958	P	38	0.006	0.449
Marthas Vineyard Airport	MA	KMVY	41.393	-70.615	P	38	0.012	0.452
Brnsbl Muni-Bman/Pol Fd Ap	MA	KHYA	41.669	-70.28	P	38	0.530	0.450
Theodore F Green State Airpor	RI	KPVD	41.723	-71.433	N	38	0.042	0.000
Bradley International Airport	CT	KBDL	41.938	-72.682	N	38	0.379	0.142
Danbury Municipal Airport	CT	KDXR	41.371	-73.483	P	30	0.004	0.259
Hartford-Brainard Airport	CT	KHFD	41.736	-72.651	N	36	0.258	0.007

Beverly Municipal Airport	MA	KBVY	42.584	-70.918	P	35	0.047	0.462
Gen E L Logan International A	MA	KBOS	42.361	-71.01	N	38	0.001	0.000
Naval Air Station	MA	KNZW	42.15	-70.933	P	21	0.786	0.078
Norwood Memorial Airport	MA	KOWD	42.191	-71.174	P	38	0.841	0.501
Concord Municipal Airport	NH	KCON	43.12	-71.3	P	34	0.534	0.476
Pease International Tradeport	NH	KPSM	43.083	-70.817	N	40	0.007	0.000
Portland International Jetpor	ME	KPWM	43.65	-70.3	N	38	0.615	0.010
Naval Air Station	ME	KNHZ	43.9	-69.933	N	37	0.395	0.000
Manchester Airport	NH	KMHT	42.933	-71.438	P	38	0.339	0.445
John F Kennedy International	NY	KJFK	40.639	-73.762	N	38	0.131	0.006
Republic Airport	NY	KFRG	40.734	-73.417	N	18	0.112	0.000
Francis S Gabreski Ap	NY	KFOK	40.844	-72.632	N	31	0.001	0.000
Bedford Hanscom Field	MA	KBED	42.47	-71.289	N	22	0.004	0.000
Lawrence Municipal Airport	MA	KLWM	42.717	-71.124	P	28	0.984	0.447
Fort Devens/Ayer	MA	KAYE	42.567	-71.6	N	18	0.405	0.007
Westover Afb/Metropolitan Air	MA	KCEF	42.2	-72.533	N	39	0.026	0.003
Barnes Municipal Airport	MA	KBAF	42.158	-72.716	P	37	0.025	0.349
Langley Afb Airport	VA	KLFI	37.083	-76.36	N	40	0.096	0.037
Simmons Aaf Airport	NC	KFBG	35.133	-78.933	N	37	0.948	0.459

Table A.7. Significance Statistics for Thunderstorm Stations

Thunderstorms

Station_Na	ST	CALL	LAT	LON	SIGN	N	MK	T
Key West International Airpor	FL	KEYW	24.555	-81.752	N	38	0.183	0.381
Key West Nas	FL	KNQX	24.583	-81.683	P	32	0.858	0.214
Miami International Airport	FL	KMIA	25.791	-80.316	P	38	0.497	0.846
Opa Locka Airport	FL	KOPF	25.907	-80.28	P	24	0.130	0.000
Fort Lauderdale Hol	FL	KFLL	26.072	-80.154	N	35	0.426	0.022
Homestead Afb Airport	FL	KHST	25.483	-80.383	N	23	0.245	0.977
Kendall-Tamiami Exec Arpt	FL	KTMB	25.648	-80.433	P	26	0.022	0.012
Palm Beach International Airp	FL	KPBI	26.685	-80.099	N	34	0.573	0.872
Ft Lauder Executive Arpt	FL	KFXE	26.197	-80.171	N	26	0.402	0.263
Melbourne Intl Ap	FL	KMLB	28.101	-80.644	P	36	0.505	0.207
Vero Beach Muni	FL	KVRB	27.653	-80.243	P	38	0.841	0.280
Pompano Beach Airpark Arpt	FL	KPMP	26.25	-80.108	P	22	0.071	0.024
Orlando International Airport	FL	KMCO	28.434	-81.325	P	38	0.191	0.114
Executive Airport	FL	KORL	28.545	-81.333	P	21	0.097	0.013
Daytona Beach Intl	FL	KDAB	29.183	-81.048	N	38	0.152	0.686
Orlando Sanford Airport	FL	KSFB	28.78	-81.244	P	29	0.002	0.000
Jacksonville International A	FL	KJAX	30.495	-81.694	N	38	0.247	0.565

Jacksonville Nas	FL	KNIP	30.233	-81.667	N	37	0.824	0.488
Mayport Naf	FL	KNRB	30.4	-81.417	P	24	0.602	0.104
Cecil Field Airport	FL	KVQQ	30.219	-81.876	N	25	0.441	0.329
Jacksonville/Craig	FL	KCRG	30.336	-81.515	P	35	0.005	0.015
Savannah/Hilton Head Intl Air	GA	KSAV	32.13	-81.21	N	34	0.050	0.972
Charleston Afb/International	SC	KCHS	32.899	-80.04	P	38	0.960	0.583
Beaufort Mcas	SC	KNBC	32.483	-80.717	P	36	0.347	0.264
Wright Aaf Airport	GA	KLHW	31.883	-81.567	P	26	0.402	0.785
St Lucie County Intl Arpt	FL	KFPR	27.498	-80.377	P	23	0.170	0.002
Albert Whitted Airport	FL	KSPG	27.765	-82.628	P	25	0.154	0.000
Page Field Airport	FL	KFMY	26.585	-81.861	N	34	0.313	0.003
Sw Florida Intn Airport	FL	KRSW	26.536	-81.755	P	27	0.868	0.053
Tampa International Airport	FL	KTPA	27.962	-82.54	N	38	0.001	0.017
Sarasota/Bradenton Intl Ap	FL	KSRQ	27.401	-82.559	N	38	0.159	0.021
St Pete-Clwtr Intl Airport	FL	KPIE	27.911	-82.688	P	38	0.037	0.005
Alma/Bacon Co.	GA	KAMG	31.536	-82.507	N	35	0.629	0.458
Malcolm Mc Kinnon Airport	GA	KSSI	31.152	-81.391	P	37	0.425	0.001
Tallahassee Regional Airport	FL	KTLH	30.393	-84.353	N	38	0.900	0.159
Gainesville Rgnl	FL	KGNV	29.692	-82.276	P	38	0.597	0.892
Valdosta Regional Airport	GA	KVLD	30.783	-83.277	N	38	0.940	0.963
Eglin Afb Airport	FL	KVPS	30.483	-86.517	P	36	0.505	0.468
Bob Sikes Airport	FL	KCEW	30.78	-86.523	P	37	0.022	0.015
Pensacola Regional Airport	FL	KPNS	30.478	-87.187	N	20	0.256	0.040
Pensacola Nas	FL	KNPA	30.35	-87.317	N	34	0.358	0.191
Whiting Field Naval Air Stati	FL	KNSE	30.717	-87.017	N	28	0.567	0.687
Panama City-Bay Co. Int Ap	FL	KPFN	30.212	-85.683	P	28	0.011	0.013
Eglin Af Aux Nr 3 D	FL	KEGI	30.65	-86.517	P	25	0.559	0.508
Wilmington Intl	NC	KILM	34.268	-77.9	N	20	0.974	0.014
Pope Afb Airport	NC	KPOB	35.174	-79.009	P	34	0.790	0.869
Fayett Rgnl/Grannis Fld Ap	NC	KFAY	34.991	-78.88	P	36	0.215	0.000
Cape Hatteras	NC	KHSE	35.233	-75.622	N	23	0.492	0.246
Seymour-Johnson Afb Airport	NC	KGSB	35.344	-77.965	P	36	0.946	0.347
Rocky Mount-Wilson Rgn Apt	NC	KRWI	35.855	-77.893	P	33	0.150	0.071
Oceana Nas	VA	KNTU	36.817	-76.033	P	33	0.053	0.000
Norfolk International Airport	VA	KORF	36.903	-76.192	N	38	0.063	0.918
Norfolk Nas	VA	KNGU	36.937	-76.289	N	38	0.821	0.137
Cherry Point Mcas	NC	KNKT	34.9	-76.883	P	35	0.000	0.004
Craven County Reg Airport	NC	KEWN	35.068	-77.048	N	37	0.472	0.816
Jacksonville	NC	KNCA	34.708	-77.44	P	32	0.062	0.001
Columbia Metropolitan Airport	SC	KCAE	33.942	-81.118	P	38	0.880	0.907
Mcentire Air National Guard S	SC	KMMT	33.967	-80.8	P	25	0.183	0.000
Florence Regional Airport	SC	KFLO	34.185	-79.724	P	36	0.989	0.097
Wallops Flight Facility Airpo	VA	KWAL	37.937	-75.471	P	18	0.150	0.018

Salisbury Ocean Cit	MD	KSBY	38.341	-75.51	N	32	0.758	0.834
Atlantic City International A	NJ	KACY	39.449	-74.567	N	33	0.085	0.487
Millville Municipal Arpt	NJ	KMIV	39.367	-75.067	P	34	0.573	0.957
Naes/Maxfield Field	NJ	KNEL	40.033	-74.35	P	21	0.833	0.401
La Guardia Airport	NY	KLGA	40.779	-73.88	P	37	0.327	0.928
Long Island Mac Art	NY	KISP	40.794	-73.102	P	37	0.990	0.903
Westchester County Airport	NY	KHPN	41.067	-73.708	N	36	0.693	0.112
Igor I Sikorsky Memorial Airp	CT	KBDR	41.158	-73.129	P	31	0.734	0.913
Groton-New London Airport	CT	KGON	41.328	-72.049	P	33	0.271	0.940
New Bedford Rgnl Airport	MA	KEWB	41.676	-70.958	P	29	0.013	0.019
Marthas Vineyard Airport	MA	KMVY	41.393	-70.615	P	24	0.006	0.001
Brnsbl Muni-Bman/Pol Fd Ap	MA	KHYA	41.669	-70.28	P	29	0.694	0.112
Theodore F Green State Airpor	RI	KPVD	41.723	-71.433	N	38	0.466	0.990
Bradley International Airport	CT	KBDL	41.938	-72.682	P	38	0.175	0.903
Danbury Municipal Airport	CT	KDXR	41.371	-73.483	P	24	0.070	0.023
Hartford-Brainard Airport	CT	KHFD	41.736	-72.651	P	33	0.566	0.917
Beverly Municipal Airport	MA	KBVY	42.584	-70.918	P	32	0.036	0.043
Gen E L Logan International A	MA	KBOS	42.361	-71.01	P	38	0.801	1.000
Norwood Memorial Airport	MA	KOWD	42.191	-71.174	N	28	0.953	0.404
Concord Municipal Airport	NH	KCON	43.12	-71.3	P	31	0.308	0.255
Pease International Tradeport	NH	KPSM	43.083	-70.817	P	26	0.103	0.995
Portland International Jetpor	ME	KPWM	43.65	-70.3	P	32	0.158	0.797
Naval Air Station	ME	KNHZ	43.9	-69.933	N	23	0.003	0.944
Manchester Airport	NH	KMHT	42.933	-71.438	P	29	0.196	0.242
John F Kennedy International	NY	KJFK	40.639	-73.762	N	38	0.393	0.896
Lawrence Municipal Airport	MA	KLWM	42.717	-71.124	P	26	0.252	0.281
Westover Afb/Metropolitan Air	MA	KCEF	42.2	-72.533	P	26	1.000	0.998
Barnes Municipal Airport	MA	KBAF	42.158	-72.716	P	28	0.396	0.105
Langley Afb Airport	VA	KLFI	37.083	-76.36	N	39	0.561	0.963
Simmons Aaf Airport	NC	KFBG	35.133	-78.933	P	35	0.932	0.842
Elizabeth City Cgas	NC	KECG	36.261	-76.175	P	19	0.484	0.105
Tyndall Afb Airport	FL	KPAM	30.067	-85.583	N	32	0.466	0.219
Hurlburt Field Airport	FL	KHRT	30.417	-86.683	N	32	0.527	0.172
Hunter Army Airfield	GA	KSVN	32.017	-81.133	N	31	0.734	0.261
Mac Dill Afb Airport	FL	KMCF	27.85	-82.517	P	30	0.498	0.790
Shaw Air Force Base	SC	KSSC	33.967	-80.467	P	36	0.138	0.584
Grand Strand Airport	SC	KCRE	33.812	-78.724	N	32	0.833	0.184
Kennedy Space Center	FL	KTTS	28.617	-80.683	P	18	0.150	0.717
Patrick Afb Airport	FL	KCOF	28.233	-80.6	P	36	0.215	0.414

Table A.8. Significance Statistics for Tropical Storm Stations

Tropical Storms								
Station_Na	ST	CALL	LAT	LON	SIGN	N	MK	T
Key West International Airpor	FL	KEYW	24.555	-81.752	P	14	0.913	0.491
Hernando County Airport	FL	KBKV	28.474	-82.454	P	8	0.536	0.369
Key West Nas	FL	KNQX	24.583	-81.683	N	11	0.533	0.503
The Fl Keys Marathon Arpt	FL	KMTH	24.726	-81.052	P	6	0.060	0.477
Miami International Airport	FL	KMIA	25.791	-80.316	P	18	0.081	0.021
Opa Locka Airport	FL	KOPF	25.907	-80.28	N	8	0.174	0.209
Fort Lauderdale Hol	FL	KFLL	26.072	-80.154	P	14	0.155	0.414
Homestead Afb Airport	FL	KHST	25.483	-80.383	N	11	0.533	0.000
Kendall-Tamiami Exec Arpt	FL	KTMB	25.648	-80.433	P	10	1.000	0.344
Palm Beach International Airp	FL	KPBI	26.685	-80.099	P	16	0.893	0.009
Charlotte County Airport	FL	KPGD	26.917	-81.991	N	8	0.108	0.250
North Perry Airport	FL	KHWO	25.999	-80.241	N	5	0.027	0.533
Naples Municipal Airport	FL	KAPF	26.152	-81.775	N	8	0.536	0.009
Ft Lauder Executive Arpt	FL	KFXE	26.197	-80.171	P	10	0.474	0.392
Melbourne Intl Ap	FL	KMLB	28.101	-80.644	P	15	0.322	0.513
Vero Beach Muni	FL	KVRB	27.653	-80.243	P	17	0.202	0.407
Pompano Beach Airpark Arpt	FL	KPMP	26.25	-80.108	P	9	0.917	0.419
Orlando International Airport	FL	KMCO	28.434	-81.325	P	16	0.964	0.485
Executive Airport	FL	KORL	28.545	-81.333	P	11	0.350	0.423
Daytona Beach Intl	FL	KDAB	29.183	-81.048	P	20	0.496	0.131
Orlando Sanford Airport	FL	KSFB	28.78	-81.244	P	13	0.024	0.399
Jacksonville International A	FL	KJAX	30.495	-81.694	P	16	0.224	0.305
Jacksonville Nas	FL	KNIP	30.233	-81.667	P	14	0.324	0.489
Mayport Naf	FL	KNRB	30.4	-81.417	N	14	0.743	0.450
Cecil Field Airport	FL	KVQQ	30.219	-81.876	P	5	0.462	0.504
Jacksonville/Craig	FL	KCRG	30.336	-81.515	P	12	0.047	0.467
Destin-Ft.Walton Beach Apt	FL	KDTS	30.4	-86.472	P	8	0.902	0.282
Savannah/Hilton Head Intl Air	GA	KSAV	32.13	-81.21	N	12	0.244	0.000
Charleston Afb/International	SC	KCHS	32.899	-80.04	P	19	0.529	0.315
Beaufort Mcas	SC	KNBC	32.483	-80.717	N	10	0.283	0.450
Wright Aaf Airport	GA	KLHW	31.883	-81.567	P	5	0.806	0.056
St Lucie County Intl Arpt	FL	KFPR	27.498	-80.377	P	11	0.350	0.456
Albert Whitted Airport	FL	KSPG	27.765	-82.628	N	13	0.669	0.339
Page Field Airport	FL	KFMY	26.585	-81.861	P	13	0.246	0.431
Sw Florida Intn Airport	FL	KRSW	26.536	-81.755	P	12	0.451	0.326
Tampa International Airport	FL	KTPA	27.962	-82.54	N	15	0.373	0.515
Sarasota/Bradenton Intl Ap	FL	KSRQ	27.401	-82.559	N	18	0.596	0.609

St Pete-Clwtr Intl Airport	FL	KPIE	27.911	-82.688	N	16	0.065	0.448
Cross City Airport	FL	KCTY	29.633	-83.105	P	8	0.902	0.506
Alma/Bacon Co.	GA	KAMG	31.536	-82.507	P	8	0.174	0.451
Malcolm Mc Kinnon Airport	GA	KSSI	31.152	-81.391	P	14	0.827	0.463
Tallahassee Regional Airport	FL	KTLH	30.393	-84.353	N	13	0.583	0.490
Gainesville Rgnl	FL	KGNV	29.692	-82.276	P	13	0.024	0.011
Valdosta Regional Airport	GA	KVLD	30.783	-83.277	P	9	0.175	0.001
Apalachicola Muni Airport	FL	KAAF	29.733	-85.033	N	8	0.536	0.522
Eglin Afb Airport	FL	KVPS	30.483	-86.517	P	14	0.228	0.404
Leesburg Regional Airport	FL	KLEE	28.821	-81.81	P	7	0.368	0.464
Bob Sikes Airport	FL	KCEW	30.78	-86.523	N	14	1.000	0.440
Pensacola Regional Airport	FL	KPNS	30.478	-87.187	N	9	0.602	0.526
Perry Foley	FL	K40J	30.072	-83.574	P	7	0.072	0.481
Pensacola Nas	FL	KNPA	30.35	-87.317	N	11	0.119	0.522
Whiting Field Naval Air Stati	FL	KNSE	30.717	-87.017	N	9	0.016	0.114
Panama City-Bay Co. Int Ap	FL	KPFN	30.212	-85.683	N	11	1.000	0.503
Eglin Af Aux Nr 3 D	FL	KEGI	30.65	-86.517	N	5	0.027	0.457
Wilmington Intl	NC	KILM	34.268	-77.9	P	13	0.502	0.382
Pope Afb Airport	NC	KPOB	35.174	-79.009	P	13	0.855	0.012
Fayett Rgnl/Grannis Fld Ap	NC	KFAY	34.991	-78.88	P	13	0.502	0.434
Michael J Smith Fld Arpt	NC	KMRH	34.734	-76.661	P	7	0.368	0.401
Cape Hatteras	NC	KHSE	35.233	-75.622	P	13	0.502	0.462
Seymour-Johnson Afb Airport	NC	KGSB	35.344	-77.965	P	10	0.592	0.511
Rocky Mount-Wilson Rgn Apt	NC	KRWI	35.855	-77.893	P	10	0.474	0.535
Oceana Nas	VA	KNTU	36.817	-76.033	P	20	0.030	0.373
Norfolk International Airport	VA	KORF	36.903	-76.192	P	22	0.499	0.003
Norfolk Nas	VA	KNGU	36.937	-76.289	P	18	0.112	0.491
Cherry Point Mcas	NC	KNKT	34.9	-76.883	P	21	0.216	0.452
Craven County Reg Airport	NC	KEWN	35.068	-77.048	P	12	0.451	0.048
Jacksonville	NC	KNCA	34.708	-77.44	P	16	0.344	0.396
Columbia Metropolitan Airport	SC	KCAE	33.942	-81.118	N	11	0.276	0.007
Florence Regional Airport	SC	KFLO	34.185	-79.724	N	11	0.533	0.452
Lumberton Municipal Arpt	NC	KLBT	34.608	-79.059	N	5	0.806	0.372
Laurinburg-Maxton Airport	NC	KMEB	34.792	-79.366	N	5	0.221	0.454
Billy Mitchell Airport	NC	KHSE	35.233	-75.622	N	14	0.381	0.359
Wallops Flight Facility Airpo	VA	KWAL	37.937	-75.471	P	10	0.032	0.517
Salisbury Ocean Cit	MD	KSBY	38.341	-75.51	P	14	0.743	0.036
Atlantic City International A	NJ	KACY	39.449	-74.567	N	14	0.274	0.465
Millville Municipal Arpt	NJ	KMIV	39.367	-75.067	N	10	0.721	0.001
Sussex County Airport	DE	KGED	38.689	-75.359	P	6	0.133	0.440
La Guardia Airport	NY	KLGA	40.779	-73.88	N	11	0.005	0.002
Long Island Mac Art	NY	KISP	40.794	-73.102	N	10	0.283	0.005
Westchester County Airport	NY	KHPN	41.067	-73.708	N	7	0.368	0.521

Igor I Sikorsky Memorial Airp	CT	KBDR	41.158	-73.129	N	10	0.107	0.004
Groton-New London Airport	CT	KGON	41.328	-72.049	N	7	0.133	0.001
Nantucket Mem	MA	KACK	41.253	-70.061	N	12	0.537	0.441
Plymouth Municipal Airport	MA	KPYM	41.91	-70.729	P	7	0.764	0.378
New Bedford Rgnl Airport	MA	KEWB	41.676	-70.958	P	6	0.133	0.440
Marthas Vineyard Airport	MA	KMVY	41.393	-70.615	P	14	0.155	0.445
Brnsbl Muni-Bman/Pol Fd Ap	MA	KHYA	41.669	-70.28	P	12	0.945	0.449
Chatham Municipal Airport	MA	KCQX	41.688	-69.993	P	5	0.462	0.406
Theodore F Green State Airpor	RI	KPVD	41.723	-71.433	N	9	0.118	0.000
Bradley International Airport	CT	KBDL	41.938	-72.682	N	8	0.019	0.009
Hartford-Brainard Airport	CT	KHFD	41.736	-72.651	P	5	0.086	0.005
Beverly Municipal Airport	MA	KBVY	42.584	-70.918	P	5	0.086	0.454
Gen E L Logan International A	MA	KBOS	42.361	-71.01	N	8	0.063	0.000
Concord Municipal Airport	NH	KCON	43.12	-71.3	P	6	0.260	0.458
Pease International Tradeport	NH	KPSM	43.083	-70.817	P	8	0.266	0.000
Portland International Jetpor	ME	KPWM	43.65	-70.3	N	7	0.035	0.055
Manchester Airport	NH	KMHT	42.933	-71.438	N	6	0.060	0.452
John F Kennedy International	NY	KJFK	40.639	-73.762	N	9	0.076	0.005
Francis S Gabreski Ap	NY	KFOK	40.844	-72.632	N	8	0.266	0.000
Bedford Hanscom Field	MA	KBED	42.47	-71.289	N	5	0.086	0.000
Westover Afb/Metropolitan Air	MA	KCEF	42.2	-72.533	P	7	0.548	0.000
Barnes Municipal Airport	MA	KBAF	42.158	-72.716	P	5	0.027	0.372
Ocean City Municipal Artp	MD	KOXB	38.308	-75.124	P	6	0.260	0.487
Langley Afb Airport	VA	KLFI	37.083	-76.36	P	17	0.711	0.000
Simmons Aaf Airport	NC	KFBG	35.133	-78.933	P	14	0.661	0.031
Elizabeth City Cgas	NC	KECG	36.261	-76.175	P	15	0.692	0.450
Tyndall Afb Airport	FL	KPAM	30.067	-85.583	N	13	0.300	0.484
Marianna Municipal Airport	FL	KMAI	30.836	-85.184	N	5	0.462	0.247
Hurlburt Field Airport	FL	KHRT	30.417	-86.683	P	11	0.213	0.444
Hunter Army Airfield	GA	KSVN	32.017	-81.133	N	14	0.274	0.487
Mac Dill Afb Airport	FL	KMCF	27.85	-82.517	P	13	0.669	0.061
Shaw Air Force Base	SC	KSSC	33.967	-80.467	N	9	0.175	0.327
Myrtle Beach Intl Airport	SC	KMYR	33.683	-78.933	P	5	0.462	0.008
Grand Strand Airport	SC	KCRE	33.812	-78.724	P	16	0.753	0.428
Nasa Shuttle Fclty	FL	KSC	28.617	-80.7	N	6	0.260	0.488
Kennedy Space Center	FL	KTTS	28.617	-80.683	P	11	0.533	0.129
Patrick Afb Airport	FL	KCOF	28.233	-80.6	P	17	0.303	0.494

References

ASCE. (2010). “Minimum design loads for buildings and other structures.” ASCE7-10, Reston, VA

Blake, Eric S, et al. *The deadliest, costliest, and most intense United States tropical cyclones from 1851 to 2010 (and other frequently requested hurricane facts)*. Miami: NOAA/National Weather Service, National Centers for Environmental Prediction, National Hurricane Center, 2011.

Blender, R., K. Fraedrich, and F. Lunkeit. "Identification of cyclone-track regimes in the North Atlantic." *Quarterly Journal of the Royal Meteorological Society* 123.539 (1997): 727-741.

Blom, Gunnar. Statistical estimates and transformed beta-variables. Diss. Almqvist & Wiksell, 1958.

Camus, Paula, et al. "Analysis of clustering and selection algorithms for the study of multivariate wave climate." *Coastal Engineering* 58.6 (2011): 453-462.

Chambers, John, William Cleveland, Beat Kleiner, and Paul Tukey, (1983), *Graphical Methods for Data Analysis*, Wadsworth.

Cheng, Linyin, et al. "Non-stationary extreme value analysis in a changing climate." Climatic change 127.2 (2014): 353-369.

Dalrymple, Tate. *Flood-frequency analyses, manual of hydrology: Part 3*. No. 1543-A. USGPO,, 1960.

Douglas, E. M., R. M. Vogel, and C. N. Kroll. "Trends in floods and low flows in the United States: impact of spatial correlation." *Journal of hydrology* 240.1 (2000): 90-105.

Emanuel, Kerry A. "An air-sea interaction theory for tropical cyclones. Part I: Steady-state maintenance." *Journal of the Atmospheric Sciences* 43.6 (1986): 585-605.

Erfani, Reza, Luc Chouinard, and Frédéric Légeron. "Reliability analysis with an icing model for estimating extreme events." *Natural Hazards* 82.1 (2016): 415-439.

Eslamian, Saeid, et al. "Application of L-moments for regional frequency analysis of monthly drought indexes." *Journal of Hydrologic Engineering* 17.1 (2011): 32-42.

FEMA (2010). Wind Retrofit Guide for Residential Buildings. Federal Emergency Management Agency, FEMA P-804

Gastineau, Guillaume, and Brian J. Soden. "Model projected changes of extreme wind events in response to global warming." *Geophysical Research Letters* 36.10 (2009).

Gomes, L., and B. J. Vickery. "Extreme wind speeds in mixed wind climates." *Journal of Wind Engineering and Industrial Aerodynamics* 2.4 (1978): 331-344.

Greenwood, J. Arthur, et al. "Probability weighted moments: definition and relation to parameters of several distributions expressable in inverse form." Water Resources Research 15.5 (1979): 1049-1054.

Hamed, Khaled H. "Trend detection in hydrologic data: the Mann–Kendall trend test under the scaling hypothesis." *Journal of hydrology* 349.3 (2008): 350-363.

Hamlet, Alan F., and Dennis P. Lettenmaier. "Effects of 20th century warming and climate variability on flood risk in the western US." Water Resources Research 43.6 (2007).

Hecht, Jory S. *Making Multi-Stakeholder Water Resources Decisions with Limited Streamflow Information*. Diss. Tufts University, 2017.

Holmes, John D. Wind loading of structures. CRC press, 2015.

Hong, H. P., and W. Ye. "Estimating extreme wind speed based on regional frequency analysis." *Structural Safety* 47 (2014): 67-77.

Hosking, Jonathan RM. "L-moments: analysis and estimation of distributions using linear combinations of order statistics." Journal of the Royal Statistical Society. Series B (Methodological) (1990): 105-124.

Huang Z. Stochastic models for hurricane hazard analysis. PhD Dissertation. Department of Civil Engineering, Clemson University, Clemson, SC, 1999.

Jakob, Dörte. "Nonstationarity in extremes and engineering design." Extremes in a Changing Climate. Springer Netherlands, 2013. 363-417.

Klein Tank, Albert, et al. "Guidelines on analysis of extremes in a changing climate in support of informed decisions for adaptation." World Meteorological Organization (2009).

Knutson, Thomas R., and Robert E. Tuleya. "Impact of CO2-induced warming on simulated hurricane intensity and precipitation: Sensitivity to the choice of climate model and convective parameterization." *Journal of climate* 17.18 (2004): 3477-3495.

Kruger, A. C., J. V. Retief, and Adam M. Goliger. "Strong winds in South Africa: Part 2 Mapping of updated statistics." *Journal of the South African Institution of Civil Engineering* 55.2 (2013): 46-58.

Kumar, Sanjiv, et al. "Streamflow trends in Indiana: effects of long term persistence, precipitation and subsurface drains." *Journal of Hydrology* 374.1 (2009): 171-183.

Leckebusch, Gregor C., et al. "Extreme wind storms over Europe in present and future climate: a cluster analysis approach." *Meteorologische Zeitschrift*17.1 (2008): 67-82.

Li, Yue, and Mark G. Stewart. "Cyclone damage risks caused by enhanced greenhouse conditions and economic viability of strengthened residential construction." Natural Hazards Review 12.1 (2010): 9-18.

Lombardo, Franklin T. "Improved extreme wind speed estimation for wind engineering applications." *Journal of Wind Engineering and Industrial Aerodynamics* 104 (2012): 278-284.

Lombardo, Franklin T., and Bilal M. Ayyub. "Analysis of Washington, DC, Wind and Temperature Extremes with Examination of Climate Change for Engineering Applications." *ASCE-ASME Journal of Risk and Uncertainty in Engineering Systems, Part A: Civil Engineering* 1.1 (2014): 04014005.

Lombardo, Franklin T., and Bilal Ayyub. "Approach to Estimating Near-Surface Extreme Wind Speeds with Climate Change Considerations." ASCE-ASME Journal of Risk and Uncertainty in Engineering Systems, Part A: Civil Engineering (2017): A4017001.

Lu, L. "Statistical methods for regional flood frequency investigations." (1992): 4095-4095.

Ma, Qing-Shan, Yan-Bao Li, and Jing Li. "Regional frequency analysis of significant wave heights based on L-moments." *China Ocean Engineering* 20.1 (2006): 85-98.

MacQueen, James. "Some methods for classification and analysis of multivariate observations." *Proceedings of the fifth Berkeley symposium on mathematical statistics and probability*. Vol. 1. No. 14. 1967.

Mardia, Kantilal V., John T. Kent, and John M. Bibby. "Multivariate analysis (probability and mathematical statistics)." (1980).

Marzban, Caren, and Scott Sandgathe. "Cluster analysis for verification of precipitation fields." *Weather and Forecasting*21.5 (2006): 824-838.

Meehl, Gerald A., et al. "Intercomparison makes a better climate model." Eos: Transactions 78 (1997): 445-446.

Milly, P. C. D., et al. "Stationarity is dead." Ground Water News & Views 4.1 (2007): 6-8.

Mishra, Vimal, et al. "Changes in observed climate extremes in global urban areas." Environmental Research Letters 10.2 (2015): 024005.

Mohamad, Ismail Bin, and Dauda Usman. "Standardization and its effects on K-means clustering algorithm." *Research Journal of Applied Sciences, Engineering and Technology* 6.17 (2013): 3299-3303.

Modarres, Reza. "Regional maximum wind speed frequency analysis for the arid and semi-arid regions of Iran." *Journal of Arid Environments* 72.7 (2008): 1329-1342.

Morgan, Eugene C., et al. "Probability distributions for offshore wind speeds." *Energy Conversion and Management* 52.1 (2011): 15-26.

Mudd, Lauren, et al. "Assessing climate change impact on the US East Coast hurricane hazard: temperature, frequency, and track." Natural Hazards Review 15.3 (2014): 04014001.

Onibon, H., et al. "Regional frequency analysis of annual maximum daily precipitation in Quebec, Canada." *Hydrological Sciences Journal/Journal des Sciences Hydrologiques* 49.4 (2004): 717-735.

Parajka, J., et al. "Seasonal characteristics of flood regimes across the Alpine–Carpathian range." *Journal of hydrology*394.1 (2010): 78-89.

Parida, B. P., R. K. Kachroo, and D. B. Shrestha. "Regional flood frequency analysis of Mahi-Sabarmati Basin (Subzone 3-a) using index flood procedure with L-moments." *Water Resources Management* 12.1 (1998): 1-12.

Peterka, J. A. "Improved extreme wind prediction for the United States." Journal of Wind Engineering and Industrial Aerodynamics 41.1-3 (1992): 533-541.

Pintar, Adam L., and Franklin T. Lombardo. "Mapping return values of extreme wind speeds." *Risk Assessment and Evaluation of Predictions*. Springer New York, 2013. 383-404.

Pujol, Nicolas, L. U. C. Neppel, and Robert Sabatier. "Regional tests for trend detection in maximum precipitation series in the French Mediterranean region." *Hydrological Sciences Journal* 52.5 (2007): 956-973.

Puvaneswaran, Manickam. "Climatic classification for Queensland using multivariate statistical techniques." *International Journal of Climatology* 10.6 (1990): 591-608.

Rousseeuw, Peter J. "Silhouettes: a graphical aid to the interpretation and validation of cluster analysis." *Journal of computational and applied mathematics* 20 (1987): 53-65.

Rosbjerg, Dan, and Henrik Madsen. "Design with uncertain design values." Hydrology in a Changing Environment, Volume Iii (1998).

Rosner, Ana, Richard M. Vogel, and Paul H. Kirshen. "A risk-based approach to flood management decisions in a nonstationary world." Water Resources Research 50.3 (2014): 1928-1942.

Salas, Jose D., and Jayantha Obeysekera. "Revisiting the concepts of return period and risk for nonstationary hydrologic extreme events." *Journal of Hydrologic Engineering* 19.3 (2013): 554-568.

Satyanarayana, P., and V. V. Srinivas. "Regional frequency analysis of precipitation using large-scale atmospheric variables." *Journal of Geophysical Research: Atmospheres* 113.D24 (2008).

Serago, J., and R.M. Vogel, Parsimonious Nonstationary Flood Frequency Analysis, *Advances in Water Resources*, 112, pp 1–16, 2018

Smithers, J. C., and R. E. Schulze. "A methodology for the estimation of short duration design storms in South Africa using a regional approach based on L-moments." *Journal of Hydrology* 241.1 (2001): 42-52.

Solomon, Susan, et al. *Climate change 2007-the physical science basis: Working group I contribution to the fourth assessment report of the IPCC*. Vol. 4. Cambridge University Press, 2007.

Stedinger, Jery R. "Fitting log normal distributions to hydrologic data." *Water Resources Research* 16.3 (1980): 481-490.

Stedinger, Jery R., and Ciprian M. Crainiceanu. "Climate variability and flood-risk management." *Risk-Based Decisionmaking in Water Resources IX*. 2001. 77-86.

Steenbergen, Raphaël DJM, Tessa Koster, and Chris PW Geurts. "The effect of climate change and natural variability on wind loading values for buildings." *Building and Environment* 55 (2012): 178-186.

Ten Brinke, W. B. M., B. A. Bannink, and Willem Ligtvoet. "The evaluation of flood risk policy in the Netherlands." Proceedings of the Institution of Civil Engineers-Water Management. Vol. 161. No. 4. Thomas Telford Ltd, 2008.

Thompson, Eric M., Laurie G. Baise, and Richard M. Vogel. "A global index earthquake approach to probabilistic assessment of extremes." *Journal of Geophysical Research: Solid Earth*112.B6 (2007).

Trepanier, Jill C. "Hurricane winds over the North Atlantic: spatial analysis and sensitivity to ocean temperature." *Natural hazards* 71.3 (2014): 1733-1747.

WMO (1988) Analysing long time series of hydrological data with respect to climate variability and change, WCAP-3, WMO-TD 224

Van den Hurk, B., et al. "KNMI climate change scenarios 2006 for the Netherlands." *KNMI scientific report WR* 1 (2006).

Vautard, Robert, et al. "Northern Hemisphere atmospheric stilling partly attributed to an increase in surface roughness." *Nature Geoscience* 3.11 (2010): 756-761.

Vogel, Richard M., and Neil M. Fennessey. "L moment diagrams should replace product moment diagrams." *Water Resources Research* 29.6 (1993): 1745-1752.

Vogel, R. M., A. Rosner, and P. H. Kirshen. "Brief Communication: Likelihood of societal preparedness for global change: trend detection." Natural Hazards and Earth System Sciences 13.7 (2013): 1773-1778.

Vogel, Richard M., Chad Yaindl, and Meghan Walter. "Nonstationarity: flood magnification and recurrence reduction factors in the United States." (2011): 464-474.

Von Storch, Hans. "Misuses of statistical analysis in climate research." *Analysis of Climate Variability*. Springer Berlin Heidelberg, 1999. 11-26.

Yang, Tao, et al. "Regional frequency analysis and spatio-temporal pattern characterization of rainfall extremes in the Pearl River Basin, China." *Journal of Hydrology* 380.3 (2010): 386-405.

Young, I. R., S. Zieger, and Alexander V. Babanin. "Global trends in wind speed and wave height." Science 332.6028 (2011): 451-455.

Yu, Insang, Jinho Kim, and Sangman Jeong. "Development of probability wind speed map based on frequency analysis." *Spatial Information Research*24.5 (2016): 577-587.